Mechanical, Hygroscopic, and Thermal Properties of Metal Particle and Metal Evaporated Tapes and Their Individual Layers

Bharat Bhushan, Zhenhua Tao

Nanotribology Laboratory for Information Storage and MEMS/NEMS, The Ohio State University, 206 W. 18th Avenue, Columbus, Ohio 43210

Received 19 June 2003; accepted 20 October 2003

ABSTRACT: Mechanical and thermal properties of magnetic tapes and their individual layers strongly affect the tribology of magnetic head–tape interface and reliability of tape drives. Dynamic mechanical analysis, longitudinal creep, lateral creep, Poisson's ratio, the coefficient of hygroscopic expansion (CHE), and the coefficient of thermal expansion (CTE) tests were performed on magnetic tapes, tapes with front coat or back coat removed, substrates (with front and back coats removed), and never-coated virgin films of the substrates. Storage modulus and loss tangent values were obtained at a frequency range from 0.016 to 28 Hz, and at a temperature range from −50 to 150 or 210°C. Longitudinal creep tests were performed at 25°C/50% RH, 40°C/25% RH, and 55°C/10% RH for 50 h. The Poisson's ratio and lateral creep were measured at 25°C/50% RH. CHE was measured at 25°C/15–80% RH. CTE values of various samples were measured at a temperature range from 30 to 70°C. The tapes used in this research included two magnetic particle (MP) tapes and two metal evaporated (ME) tapes that were based on poly(ethylene terephthalate) and poly(ethylene naphthalate) substrates. The master curves of storage modulus and creep compliance for these samples were generated for a frequency range from 10^{-20} to 10^{15} Hz. The effect of tape manufacturing process on the various mechanical properties of substrates was analyzed by comparing the data for the substrates (with front and back coats removed) and the never-coated virgin films. A model based on the rule of mixtures was developed to determine the storage modulus, complex modulus, creep compliance, and CTE for the front coat and back coat of MP and ME tapes. © 2004 Wiley Periodicals, Inc. J Appl Polym Sci 92: 1319–1345, 2004

Key words: magnetic tape; rule of mixtures; storage modulus; creep; Poisson's ratio

INTRODUCTION

Magnetic tapes provide extremely high volumetric density, high data rates, and low cost per megabyte compared to those of other storage media. These are primarily used for data backup and some high volumetric density recording devices such as instrument and satellite recorders.[1] For example, the Generation 4 Ultrium format LTO (Linear Tape Open) tape provides for up to 1.6 TB in a single cartridge, with a compressed data rate of up to 320 MB/s.[2] The high volumetric density is achieved by a combination of high areal density and the use of an ultrathin tape. This requires that the substrate and the finished tape be mechanically and environmentally stable in both the longitudinal (for high linear density) and lateral (for high track density) directions. Ever increasing recording density requires a better understanding of the dimensional stability of the tape, especially of the polymeric substrate that takes 75 to 95% of the total thickness. As a way to minimize stretching and damage during manufacturing and use of thin magnetic tapes, the substrate should be a high-modulus, high-strength material with low viscoelastic and shrinkage characteristics. Also, because high coercivity magnetic films on metal evaporated (ME) tapes are deposited and heat treated at elevated temperatures, an ME substrate with stable mechanical properties up to a temperature of 100–150°C or even higher is desirable.[1]

The first author's group extensively studied the viscoelastic properties and dimensional stability of ultrathin polymeric films and tapes.[1,3–12] This includes the creep, shrinkage, dynamic mechanical behavior, Poisson's ratio, thermal and hygroscopic expansion of polymeric substrates, tapes, and stripped tapes without front coat and/or back coat. Weick and Bhushan,[5,6] Ma and Bhushan[11,12] modeled the magnetic tape as a three-layer composite: front coat, substrate, and back coat. By performing tests on the combined layers and applying the rule of mixtures, storage modulus, complex modulus, lateral creep compliance, and coefficient of thermal expansion of each individual

Correspondence to: B. Bhushan (bhushan.2@osu.edu).

Contract grant sponsor: Nanotribology Laboratory for Information Storage and MEMS/NEMS (NLIM) at The Ohio State University.

Journal of Applied Polymer Science, Vol. 92, 1319–1345 (2004)

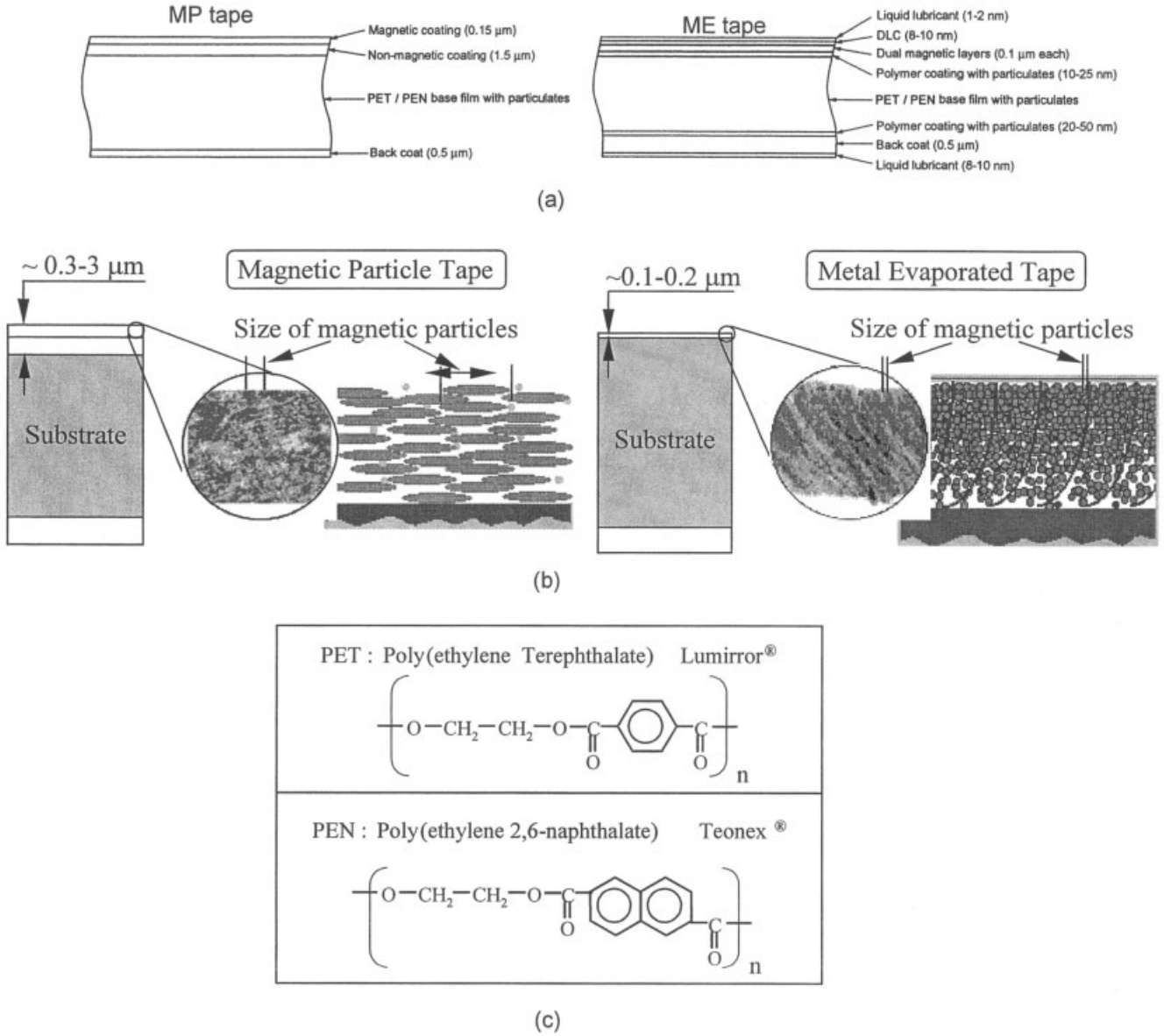

Figure 1 Magnetic tape: (a) schematic diagram of MP and ME tapes; (b) detailed construction of MP and ME tapes (downloaded from http://www.sony.co.jp/en/Products/METape/eng/why/index.html, and slightly modified); (c) chemical unit structures of various polymeric films.

layer were obtained. To date, longitudinal creep compliance of individual layers has not been measured. There is another key concern to tape and substrate manufacturers, which is the degradation of the substrate during the tape manufacturing. Such information is useful for designers to develop future magnetic tapes that use thinner and highly stable materials.

The objective of this study was to measure longitudinal creep compliance of magnetic tapes and their individual layers, as well as to study the effect of tape manufacturing processing on the longitudinal creep compliance of substrates. Other data reported are dynamic mechanical analysis (DMA) data, lateral creep compliance, Poisson's ratio, and coefficient of hygroscopic and thermal expansion. Two magnetic particle (MP) and two ME tapes, each of which used two typical polymeric substrates, poly(ethylene terephthalate) (PET) and poly(ethylene naphthalate) (PEN), and corresponding never-coated virgin films, were studied.

EXPERIMENTAL

Test samples

Magnetic tapes selected for this study are shown in Figure 1(a) and (b). These tapes are representative of the two basic types of MP tapes in which magnetic

TABLE I
Sample Matrix: Symbols and Thickness (μm)

Width (mm)	Tape	Substrate + front coat	Substrate + back coat	Substrate	Never-coated substrate film[a]
12.67	MP-DLT	MP-DLT/SF	MP-DLT/SB	MP-DLT/S	T-PET(2)
	8.9	~ 8.6	~ 6.5	6.1	6.1
12.67	MP-LTO			MP-LTO/S	T-PEN
	8.9			6.1	6.1
8	ME-Hi8	ME-Hi8/SF	ME-Hi8/SB	ME-Hi8/S	T-PET(3)
	10.46	~ 10.06	~ 10.3	9.9	9.9
6.35	ME-MDV			ME-MDV/S	T-PEN(2)
	5.26			4.7	4.7

[a] T-PEN corresponds to the sample in Refs. 7 and 8. T-PEN(2), T-PET(2), and T-PET(3) correspond to the sample in Ref. 11.

particles are dispersed in a polymeric binder; and ME tapes in which continuous films of magnetic materials are deposited onto the substrate using vacuum techniques. Both of the MP tapes used in this study, MP-DLT with 6.1 mm PET substrate and MP-LTO with 6.1 mm PEN substrate, have a total thickness of 8.9 mm. The substrate for ME-Hi8 is 9.9 mm thick PET, and that for ME-MDV is 4.7 mm thick PEN.

PET and PEN films are commonly used as magnetic tape substrates, and have been widely studied.[1,7,8,10,13] Their chemical molecular structures are shown in Figure 1(c). The glass-transition temperatures (T_g) for the PET and PEN substrates are about 80 and 120°C, respectively.[8,10,13] The typical crystallinities for PET and PEN films are about 40–50 and 30–40%, respectively.[8] Information about the specific chemistry of the materials used in the front coats and back coats is not available from the manufacturers. However, based on Bhushan,[1] the front coat may consist of a single magnetic layer, as in the cases of single-layer MP tapes. Their composite magnetic layers consist of magnetic particles, a polymer binder, and a lubricant. The MP tape magnetic layer also consists of abrasive (mostly alumina) and conductive carbon particles. The front coat may also consist of a magnetic layer and a nonmagnetic polymer underlayer, as in the case of double-layer MP tape. For ME tapes, the front coat consists of a magnetic layer, a diamond-like carbon coating (DLC), and a lubricant layer. The ME tape magnetic layer is a continuous thin film of Co—Ni—O deposited by evaporation. The back coat consists of carbon black in a polymeric binder.

The symbols of the samples are listed in Table I. They include the following layer formats:

- Magnetic tapes as cut from the cassettes
- Substrates (front coat and back coat removed) (S)
- Substrate plus front coat (back coat removed) (SF)
- Substrate plus back coat (front coat removed) (SB)
- Never-coated virgin substrate film

To obtain the substrate for the MP tapes, methyl ethyl ketone (MEK) was used to remove the front coat and back coat. This involved placing the tape on a flat piece of glass and rubbing both sides of the tape longitudinally with a paper towel saturated with MEK until only the transparent PET substrate remained. The substrate for the ME tape was obtained in a similar manner. However, MEK could be used to remove only the back coat of the ME tape. A 2% hydrochloric acid solution was used to remove the front coat. This procedure involved dipping the ME tape into the solution until the metal-evaporated coating could be rubbed off.

Removing the back coat of the MP and ME tapes without removing the front coat involved spreading a thin bead of distilled water on a glass plate. The tape specimen was then placed front coat down in this bead of water. All excess water around the edges of the tape was soaked up with a paper towel. The back coat could then be carefully removed using MEK, and the thin film of polar water molecules between the glass plate and front coat of the tape helped prevent the nonpolar MEK molecules from dissolving the front coat. Removing the front coat on the MP and ME tapes without removing the back coat involved the same procedure. All the samples were left in ambient condition (24–26°C, 30–60% RH) for at least 4 days before testing.

Test apparatus and procedure

DMA tests

A Rheometrics (Piscataway, NJ) RSA II dynamic mechanical analyzer was used to measure the dynamic mechanical properties of the polymeric films.[1,8,12] The analyzer was used in an autotension mode with a static force (~ 0.25% strain in this study) on the samples to prevent the thin films from buckling during application of the dynamic strain. Rectangular samples [6.35 × 22.5 mm (width × length)] were used. In this mode, samples are fastened vertically between the grips and a sinusoidal strain is applied to the specimen, and the corresponding sinusoidal load on the sample is measured by a load cell. Frequency/temper-

ature sweep experiments were performed for a 0.1 to 182 rad s^{-1} (0.016 to 28 Hz) range, and 14 data points were taken for each frequency sweep at 11 different temperature levels ranging from −50 to 150°C for the PET films and corresponding tapes, and 14 temperature levels ranging from −50 to 210°C for PEN films and corresponding tapes. The temperature increment was 20°C, and the soak time for each temperature level was 10 s. For PET and PEN films, the upper limits for test temperatures were selected to cover the peak temperatures for loss tangent related to glass-transition temperatures.

Because the polymeric films are viscoelastic, there will be a phase lag between the applied strain and the measured load (or stress) on the specimen. The storage modulus E' is therefore a measure of the component of the complex modulus, which is in phase with the applied strain, and the loss modulus E'' is a measure of the component that is out of phase with the applied strain. The in-phase stress and strain result in elastically stored energy that is completely recoverable, whereas out-of-phase stress and strain result in the dissipation of energy, which is nonrecoverable and is lost to the system. The loss tangent tan δ is simply the ratio of the loss modulus to the storage modulus.[1] Equations used to calculate the storage (or elastic) modulus E' and loss tangent tan δ are as follows:

$$E' = \cos\delta\left[\frac{\sigma}{\varepsilon}\right] \tag{1}$$

$$E'' = \sin\delta\left[\frac{\sigma}{\varepsilon}\right] \tag{2}$$

$$|E^*| = \sqrt{(E')^2 + (E'')^2} \tag{3}$$

$$\tan\delta = \frac{E''}{E'} \tag{4}$$

$$\varepsilon = \frac{D}{L} \quad \sigma = FgK_\sigma \tag{5}$$

where E' is the storage modulus, E'' is the loss (or viscous) modulus, E^* is the magnitude of the complex modulus, ϵ is the applied strain, σ is the measured stress, δ is the measured phase angle shift between stress and strain, D is the displacement from the strain transducer, K_σ is a stress constant equal to 100/(width × thickness of the sample),[14] L is the length of the sample, g is the gravitational constant (9.81 m s^{-2}), and F is the measured force on the sample from the load cell. The T-PET(2) sample was measured a number of times to check for the reproducibility. Reproducibility of E' and loss tangent was found to be about ±5 and ±3%, respectively.

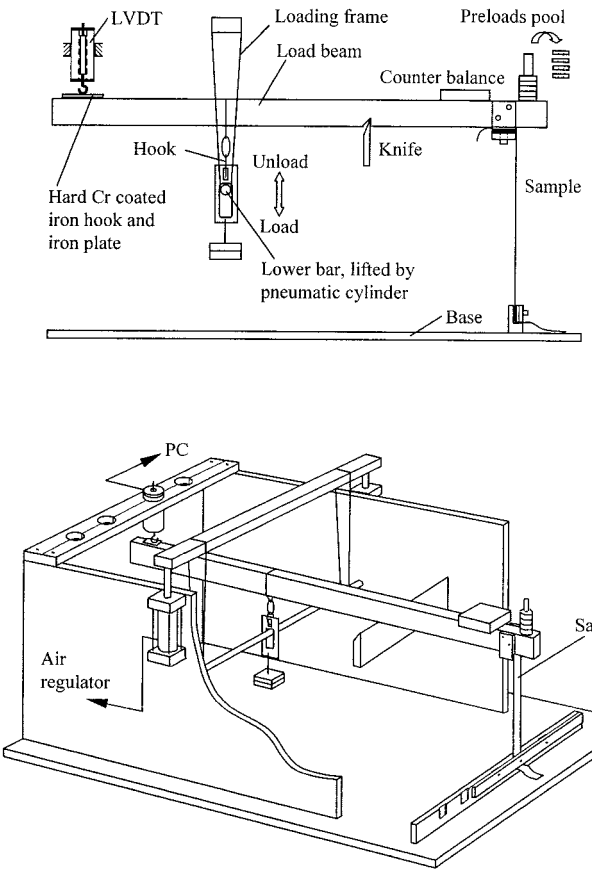

Figure 2 Schematic of creep test apparatus.[10]

Longitudinal creep tests

Long-term creep characteristics of tape samples were evaluated using the test apparatus shown in Figure 2.[7,10] The apparatus was placed in an environmental chamber to measure the properties of interest at elevated temperature and/or humidity levels. The apparatus consisted of four load beams (only one is schematically shown in Fig. 2) placed on a knife edge; by using four beams, four samples can be measured at a time. The film sample was vertically attached between one end of the load beam and the base. The load beam was adjusted on the knife in the lateral direction to keep the sample straight in the vertical direction. A linear variable differential transformer (LVDT) was connected to the other end of the load beam to measure deflection attributed to the creep deformation of the film sample, and the output was recorded on a personal computer (PC). The load was remotely applied on the load arm using a pneumatically controlled mechanism, given that the apparatus was placed in an environmental chamber. The dead weight was attached to a ring that was connected to a hook placed on the load beam. The ring was moved up or down in the vertical direction by moving the loading frame pneumatically, so that the hook was released or

engaged, and the dead weight was removed from or applied to the load beam, respectively. A counterbalance load was applied near the sample end to have no load on the sample before a desired load was attached. The load experienced by the sample was calibrated by placing a weight on the load beam at the sample clamp region while the load beam was flat, for a range of loads on the other end. The LVDT reading was also calibrated by directly measuring the displacement at the sample end using a micrometer gauge, and comparing that to the LVDT reading.

The virgin substrate samples were cut into 190 $\times$12.7-mm ($\frac{1}{2}$-in.) strips to accommodate the creep apparatus, and the width of all other samples was the same as that of the tape from which the sample came. Resulting strain was determined by measuring the change in length of the samples relative to their original length. Before attaching the samples, the environmental chamber was turned on to stabilize the temperature and humidity and allow the creep test apparatus to be conditioned for 1 h. The samples were then attached and conditioned at a preset temperature, without any load, for 1 h. Next, a preload of 0.5 MPa was applied to the samples by removing a corresponding weight from the pool of preloads, and then the samples were conditioned for stabilization in an environmental condition. During this stabilization period of typically 2 h, the output signals were monitored until they were steady. The conditioning procedure, for instance, has an effect on the creep behavior that the sample has lost its long-term memory and currently remembers loads applied in its immediate past history.[15] All creep tests were performed at a constant load of 7 MPa. This stress value was chosen because it is a typical stress applied to tapes in tape drives during use, and has been shown to keep the creep deformation in the linear viscoelastic regime.[1] Given that 55°C is the upper limit of the operating envelop for magnetic tapes, the maximum temperature used for creep experiments was 55°C. The long-term creep measurements were performed at 25, 40, and 55°C for a period of 50 h, uncontrolled humidity (50 to 60% RH, 15 to 25% RH, and 5 to 10% RH, respectively). Short-term creep measurements were also reported at 12 min. Creep measurements were made in the machine direction (MD) of the films because stress is applied along the MD direction during operation and in a wound reel for a magnetic tape, which corresponds to the MD of the substrate films.[7]

Equations used to calculate the strain $\epsilon(t)$ and creep compliance $D(t)$ are as follows:

$$\varepsilon(t) = \frac{\Delta l(t)}{l} \tag{6}$$

and

$$D(t) = \frac{\varepsilon(t)}{\sigma} = \frac{\Delta l(t)}{\sigma l} \tag{7}$$

where $\Delta l(t)$ is the change in length, l is the original length, and σ is the constant applied external stress.

Poisson's ratio, lateral creep, and hygroscopic expansion

Figure 3(a) shows the schematic diagram of the experimental apparatus developed to conduct the Poisson's ratio measurement.[9–11] An opaque sample, 280 mm long and 12.7 mm wide, loaded at one end, and fixed to a microgauge at the other end, was wrapped over a curved quartz glass (85 mm radius). The polymeric substrate was sputter coated with a gold coating ($\sim$ 5 nm thick), so that it was opaque and measurement could be made. The laser scan micrometer (LSM) system (transmitter, LS5041T; receiver, LS5041R; and controller, LS5501; Keyence Corp., Osaka, Japan), with an absolute accuracy of 2 μm and a resolution of 0.05 μm, was used to measure the changes in the width of the sample. Figure 3(b) shows details of the measurement area. The curved glass supports the sample and prevents puckering in the transverse direction (TD) under a longitudinal stress. To achieve this, the sample should have good contact with the curved glass at least at the measurement point. On the other hand, the polymer film tends to stick to the curved glass, especially when the humidity is high. This induces extra static friction force, and prevents the uniform distribution of the stress over the length of the sample. In this work, the sample maintained a "line" contact with the curved glass by control of the contact angle at approximately 3–5°.

The experimental apparatus was placed inside a chamber [Fig. 3(d)] where temperature and relative humidity were controlled at 25 $\pm$ 0.5°C and 50 $\pm$ 2% RH, respectively. Airflow inside the chamber was also controlled so that air did not blow directly onto the sample while maintaining uniform environmental conditions inside the chamber. The sample was preloaded to a normal load of 0.5 MPa. After the temperature and humidity reached the desired values, the sample was conditioned for another 30 min before the test was started. Calibration tests showed that, under a stress of 0.5 MPa, the lateral dimensional change of the sample after 30 min for a period of 20 h was within 0.2 μm, less than 0.0016% lateral strain. So the samples could be regarded as having reached equilibrium after 30 min of conditioning.

The LSM was composed of various materials that change dimension according to the environmental condition. The scanning position of the laser beam was determined by the refractive index of the atmosphere and lens, which was also affected by the temperature

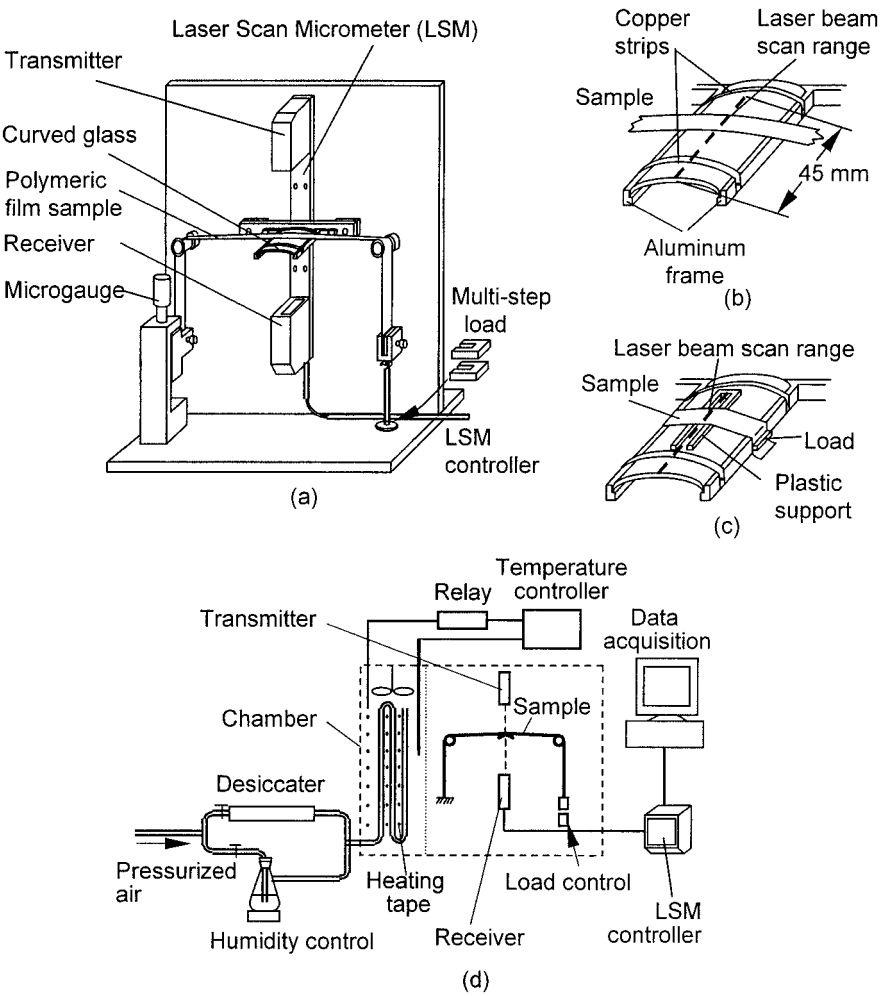

Figure 3 Schematic of (a) lateral profile measurement apparatus, (b) details of the curved glass for lateral profile measurement, (c) details of the curved glass with a plastic support for hygroscopic/thermal expansion measurements, and (d) functional block diagram of the measurement system.[11]

and humidity. In this work, an aluminum foil sample (15.4 μm thick; Reynolds, Columbus, OH) was used to calibrate the systematic error. The foil was slit to about 12.1 mm width. Figure 4 shows the measurement results of the width of the Al sample affected by the change of temperature and humidity. The CTE of Al foil is known to be 23.6×10^{-6}/°C for 25 to 50°C. Thus a 12.1-mm sample should expand 4.3 μm from 25 to 40°C. The measurement shows a 3.1 $\pm$ 0.1 μm expansion, so there is a -1.2 μm systematic error. To confirm that systematic error is the same for various samples and to determine the accuracy of the measurement, the thermal expansion of a standard polycrystalline alumina (99.5%) rod sample (10 mm diameter) was measured at the same conditions (25–40°C), whereas the humidity remained constant at 50% RH. A support was used to hold the rod sample over the curved glass. The measured expansion was -0.5 ± 0.1 μm, whereas the theoretical value should be 0.7 μm. Thus the systematic error of the LSM was confirmed as -1.2 μm when the temperature changed from 25 to 40°C and the relative humidity was maintained constant at 50%. This systematic error was also confirmed by the manufacturer. The accuracy and repeatability in the width change was established to be ± 0.1 μm from these tests on aluminum and alumina samples. Similarly, the LSM has a systematic error of about 0.4 μm when the relative humidity changes from 15 to 80% RH at 25°C (Fig. 4). These errors were subtracted out in the experiments when the measurements for different conditions were compared. The measured fluctuation at a given condition is about ± 0.1 μm in Figure 4. This is taken as the relative accuracy of the measurement of the change in width.

Poisson's ratio and short-term creep behavior. For the measurement of Poisson's ratio, the sample was loaded in steps over a load range, say from 5 to 42 MPa at a step interval of 7 MPa.[9,11] At each load level, the sample was held for 12 min to stabilize the measurement. The width profile was measured by moving

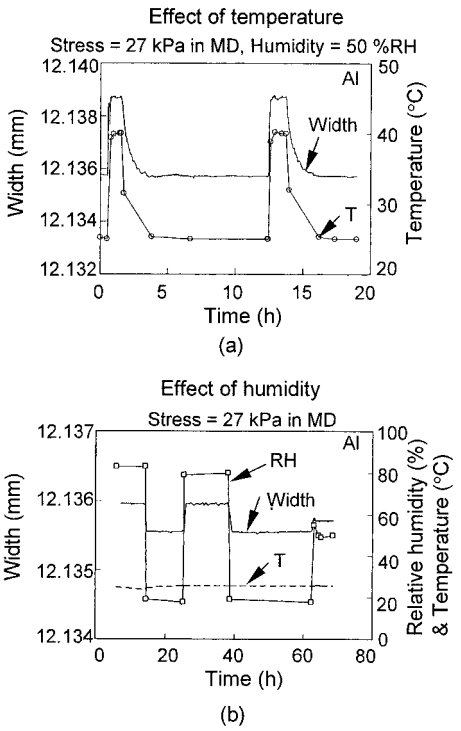

Figure 4 Effect of (a) temperature and (b) relative humidity on the width change of Al foil sample for calibration of the test apparatus. "T" and "RH" represent temperature and relative humidity, respectively.[11]

the sample in the longitudinal direction at a speed of 10 μm/s [for an example see Fig. 5(a)]. By comparing the profiles at different load levels, and matching the position of the characterized features, the lateral and longitudinal displacements of the sample at the corresponding stress were obtained. Thus the longitudinal and lateral deformation and Poisson's ratio were calculated as follows:

$$\nu = \frac{\varepsilon_\perp}{\varepsilon_\parallel} = \frac{\Delta w/w}{\Delta l/l} = \frac{\Delta w l}{\Delta l w} \tag{8}$$

where ν is the Poisson's ratio; $\epsilon_\perp$ and $\epsilon_\parallel$ are the lateral contraction and longitudinal elongation, respectively; w and Δw are the sample width and the decrease of the width; l and Δl are the sample lengths from the microgauge to the measuring point and the increase of the length, respectively. Figure 5(b) shows the longitudinal elongation, lateral contraction, and corresponding Poisson's ratio for MP-DLT tape (described below) at 25°C, 50% RH. The results show a good linear relationship.

Long-term lateral creep behavior. For measurement of long-term lateral creep behavior, the sample was conditioned at 0.5 MPa for 1 h, and loaded at another 7 MPa for 50 h.[9,11] The width profiles were measured at various time periods. By comparing the profiles and matching the position of the characteristic features, the lateral contraction and longitudinal elongation at various times were recorded.[11] For both Poisson's ratio and creep measurement, the nominal test conditions were set as 25°C, 50% RH. Figure 6(a) and (b) show typical long-term deformation of T-PET(2) (described below) raw film.

Hygroscopic expansion. There is no corresponding ASTM standard for measuring the CHE for polymeric film. The most commonly used method is according to the Technical Association of the Pulp and Paper Industry (TAPPI) Useful Method 549, like Neenah Multiple Specimen Paper Expansimeter (Adirondack Machine Corp., Glens Falls, NY).[1] The typical reading accuracy for this expansimeter is ± 13 μm, over a sample size of 127 mm (up to 254 mm), which converts to a relative accuracy of $\pm 10^{-4}$ for the measurement. The LSM technique has an extreme high accuracy, as ± 0.1 μm for a typical sample size of 12.7 mm (up to 40

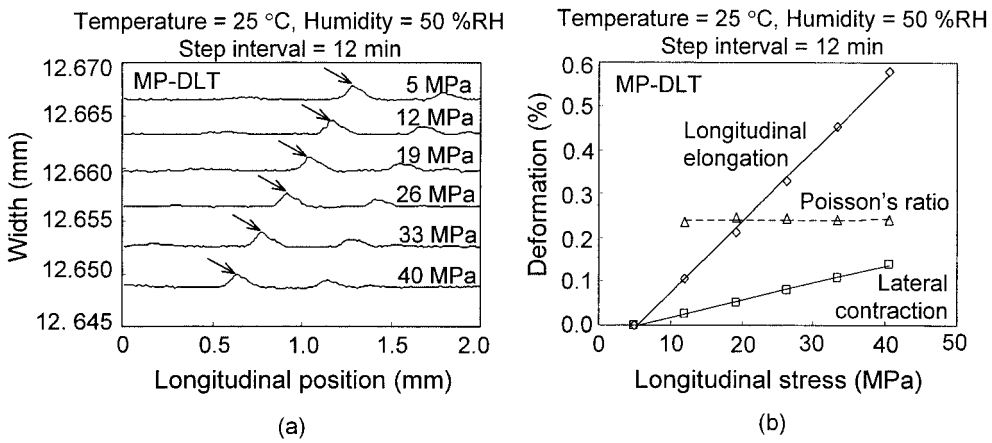

Figure 5 (a) Width profiles of MP-DLT tape at various stresses. Arrows indicate a typical feature in the profile. Profile matching, by calculating the shifting of a feature, was used to obtain (b) longitudinal elongation, lateral contraction, and Poisson's ratio.[11]

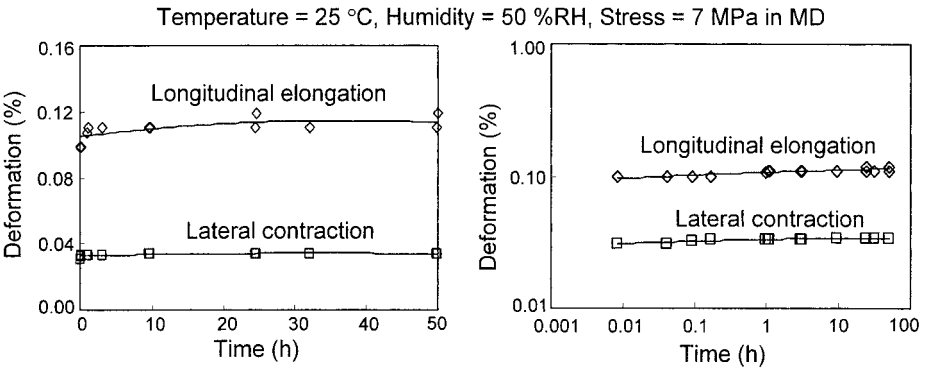

Figure 6 Longitudinal elongation and lateral contraction of T-PET(2) film.[11]

mm of accurate scanning range), which corresponds to $\pm 10^{-5}$ relative accuracy for the measurement, which is higher than that of the expansimeter method.[9,11]

Figure 3(c) shows the details of the sample and curved glass, set for CHE measurements. A 42 × 12.7 mm (length × width) sample was loaded in the machine direction (MD). The dimension in the transverse direction (TD) of the sample was measured as the humidity changed from 15 to 80% RH, whereas the temperature was controlled at 25 ± 0.5°C. The CHE in TD was thus obtained. The load was about 50 kPa, within the range recommended by ASTM E831-93 and D696-98 standards,[16] and is not supposed to result in significant creep of the sample during the test. The reproducibility of the technique was found to be within 0.5×10^{-6}/% RH. Two hygroscopic cycles were carried out on each sample.

Thermal expansion tests

The LSM apparatus was also used to measure the CTE.[9] However, the temperature range limited by the LSM was below 45°C. Over such a small temperature range, the measurement error should be large, and does not provide reliable data. Instead, a commercially available standard thermomechanical analysis (TMA) device TA2940 (TA Instruments, New Castle, DE) is commonly used and was used in this study to measure CTE.[10–12] In this instrument, the sample was mounted between a static stage and a floating probe and heated with a heater. The dimensional change of the sample was recorded by the LVDT. The force applied on the sample was controlled by the stepper motor and corresponding load control. The typical sample size in this study was 3 × 40 mm; after clipping, the gauge length of the sample was approximately 25.5 mm. For the samples cut in the TD of tapes, the sample length was 12.67 mm and the gauge length was about 8.7 mm. The temperature ranged from 10°C (precooled) to 70°C, at a heating rate of 3°C/min. A constant 3*g* force was applied to the sample to keep it flat and stable.

After the dimensional change of the sample was measured, it was converted to the CTE as

$$\alpha = \frac{\Delta l}{l \Delta T} \tag{9}$$

where Δl and l are length change and the original length at 10°C and ΔT is the temperature range. According to ASTM E831-93,[16] the measured CTE during the first 20° of the test (10–30°C) was regarded as unstable, and was not used in the discussion in this study. The data were then converted by replacing the original length in eq. (9) to the length at 30°C, so that the data would coincide with zero expansion at 30°C. Aluminum foil [15.4 μm thick; CTE = 23.6×10^{-6}/°C (Reynolds)] was used to calibrate the instrument. The results of three repeated tests on this foil were 23.6, 23.4, and 23.6×10^{-6}/°C. The TMA was thus proved to have a good repeatability.

Rule-of-mixtures approach

Because magnetic tapes consist of multiple layers, they resemble polymer composite laminates.[5,6,11,12] Generally they can be regarded as a three-layer composite as shown in Figure 7. The rule-of-mixtures method can be used to predict the elastic mechanical properties of

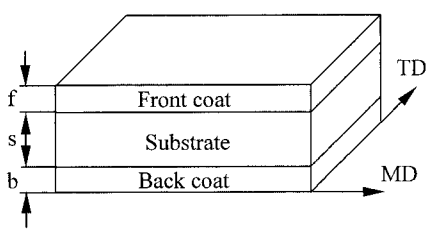

Figure 7 Nomenclature used for rule-of-mixtures equations.

the whole tape if the data for each layer are known, assuming that there is perfect bonding between each layer, that is, assuming isostrain.[17] Based on this rule

$$\sigma_t A_t = \sigma_f A_f + \sigma_s A_x + \sigma_b A_b \tag{10}$$

where σ_t, σ_f, σ_s, and σ_b are the stresses in the entire tape, front coat, substrate, and back coat, respectively. A_t, A_f, A_s, and A_b are the cross-sectional areas of the tape, front coat, substrate, and back coat, respectively. And

$$E_t t = E_f f + E_s s + E_b b \tag{11}$$

where E_t, E_f, E_s, and E_b are the Young's moduli of the tape, front coat, substrate, and back coat, respectively; and t, f, s, and b are the thicknesses of the corresponding layers.

For any two combined layers, similar equations apply, such as

$$E_{fs}(f + s) = E_f f + E_s s \tag{12}$$

where E_{fs} is the Young's modulus of the combined layers of substrate plus front coat.

If we know two of the moduli in eq. (12), for example E_{fs} and E_s, and the thickness of each layer, we can calculate the third modulus, say E_f.

The creep compliance relationship between layers for the tape can also be deduced from eqs. (7) and (10) as

$$\frac{t}{D_t} = \frac{f}{D_f} + \frac{s}{D_s} + \frac{b}{D_b} \tag{13}$$

where D_t, D_f, D_s, and D_b are the creep compliances for the tape, front coat, substrate, and back coat, respectively.

As was done for the three-layer case, one can determine equations for the compliance of the front coat in terms of the measured compliance values for the combined front coat and substrate as well as the substrate itself:

$$\frac{f + s}{D_{fs}} = \frac{f}{D_f} + \frac{s}{D_s} \tag{14}$$

where D_{fs} is the creep compliance of the combined front coat and substrate.

RESULTS AND DISCUSSION

DMA results

Figure 8(a)–(d) show representative storage moduli and loss tangents as a function of frequency and temperature for various materials.[12] High storage modulus indicates high elastic stiffness. From the three-dimensional surface representations of storage modulus, it can be seen that higher elastic moduli correspond to higher deformation frequencies and lower temperatures. High loss tangent indicates greater viscoelastic behavior of the material, or that more energy is dissipated during the deformation. For a general comparison, Table II summarizes the storage moduli of various samples at 0.016 and 28 Hz, 25°C.

In Figure 8(a), the storage moduli of the five MP-DLT samples show a similar trend, that is, the rate of decrease of storage moduli as a function of temperature is low before it reaches about 70°C; then the rate suddenly increases and storage moduli decrease to a low level, as the material transits from a glassy to a rubbery state. This change corresponds to the character of the loss tangents in Figure 8(b), where the loss tangent remains low below 70°C, indicating that a small amount of energy is dissipated, after which the loss tangent begins to rise at 70–90°C and peaks at 110–130°C. These tendencies and critical temperatures are identical in all the MP-DLT samples including tape, combined layers, substrate, and the virgin film T-PET(2). This demonstrates that the dynamic mechanical property of magnetic tape is generally governed by its substrate material.

By comparing the details of loss tangent data for MP-DLT samples in Figure 8(b), it can be seen that the data for the tape are slightly higher than those for the substrate, covering a wide vertical range as the frequency changes, especially at temperatures close to T_g. This makes the onset temperature [extrapolation of the loss tangent curve at maximum slope, as shown in Fig. 8(b)] for MP-DLT tape lower than that for the substrate, although the peak temperatures of the loss tangent for these two samples are still the same. The magnitude of loss tangent for the tape is higher than that for the substrate when the temperature is below T_g. Thus, the MP-DLT tape shows slightly higher viscoelastic behavior than that of the substrate. It should be noted that the magnetic tape can be regarded as a multilayer composite. The energy dissipated during the sinusoidal loading comes not only from its composing materials, but also from the interface.

The statement that the dynamic mechanical property of magnetic tape is governed by its substrate material also applies to the ME-Hi8 sample [Fig. 8(c) and (d)], although the storage moduli for ME tapes were found to be higher than that for the substrate. For ME tapes, no obvious difference was found between the loss tangents for tapes and for their substrates.

By comparing the storage moduli data for MP-DLT and ME-Hi8, it can be seen that the storage moduli for MP samples in a wide range of frequencies are higher than those for ME samples. For example, the storage moduli for the MP-DLT tape and substrate at 30°C, 28 Hz were 8.2 and 7.8 GPa, respectively, whereas the cor-

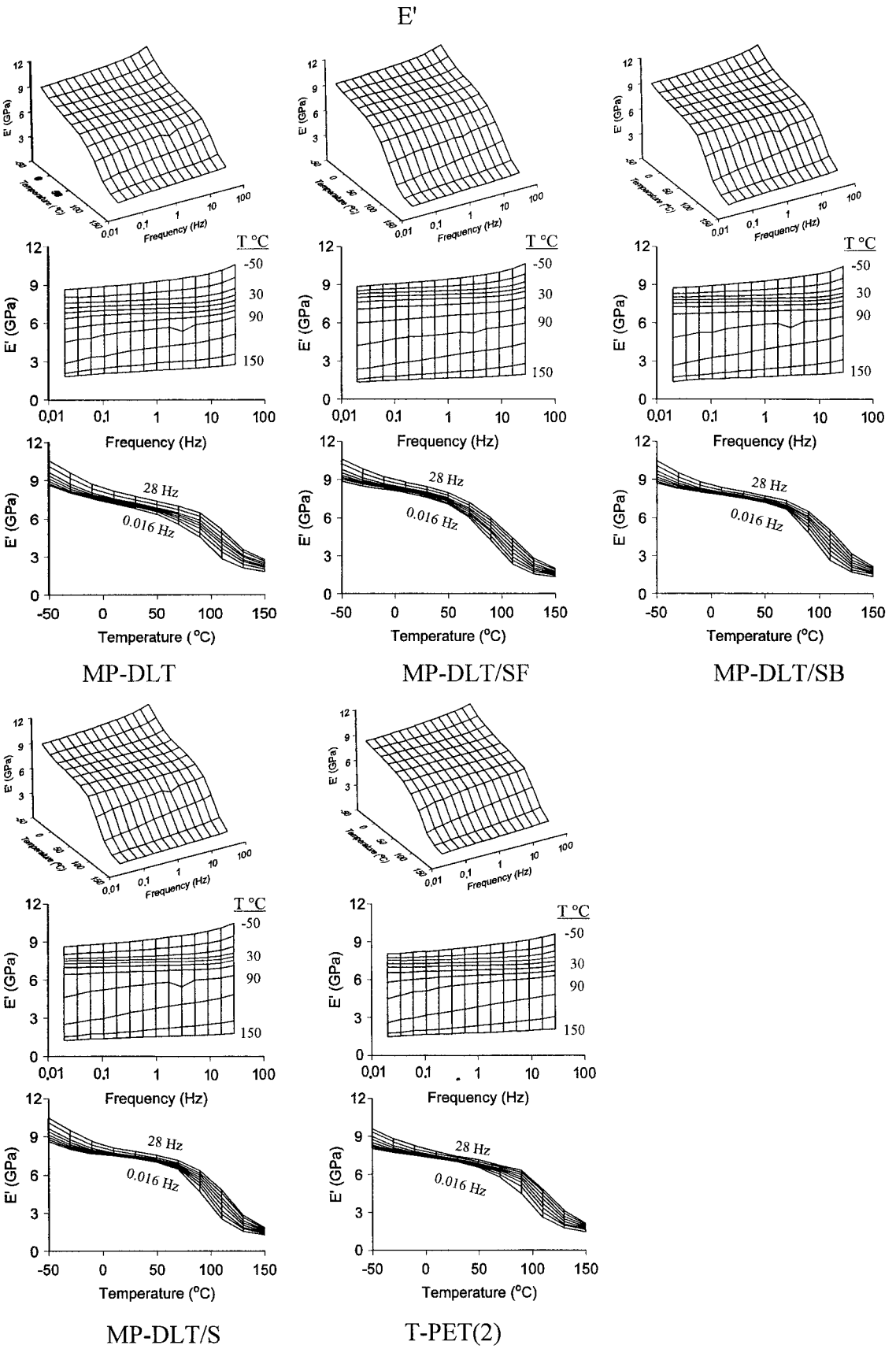

Figure 8 Dynamic mechanical analysis data on MP-DLT and ME-Hi8.

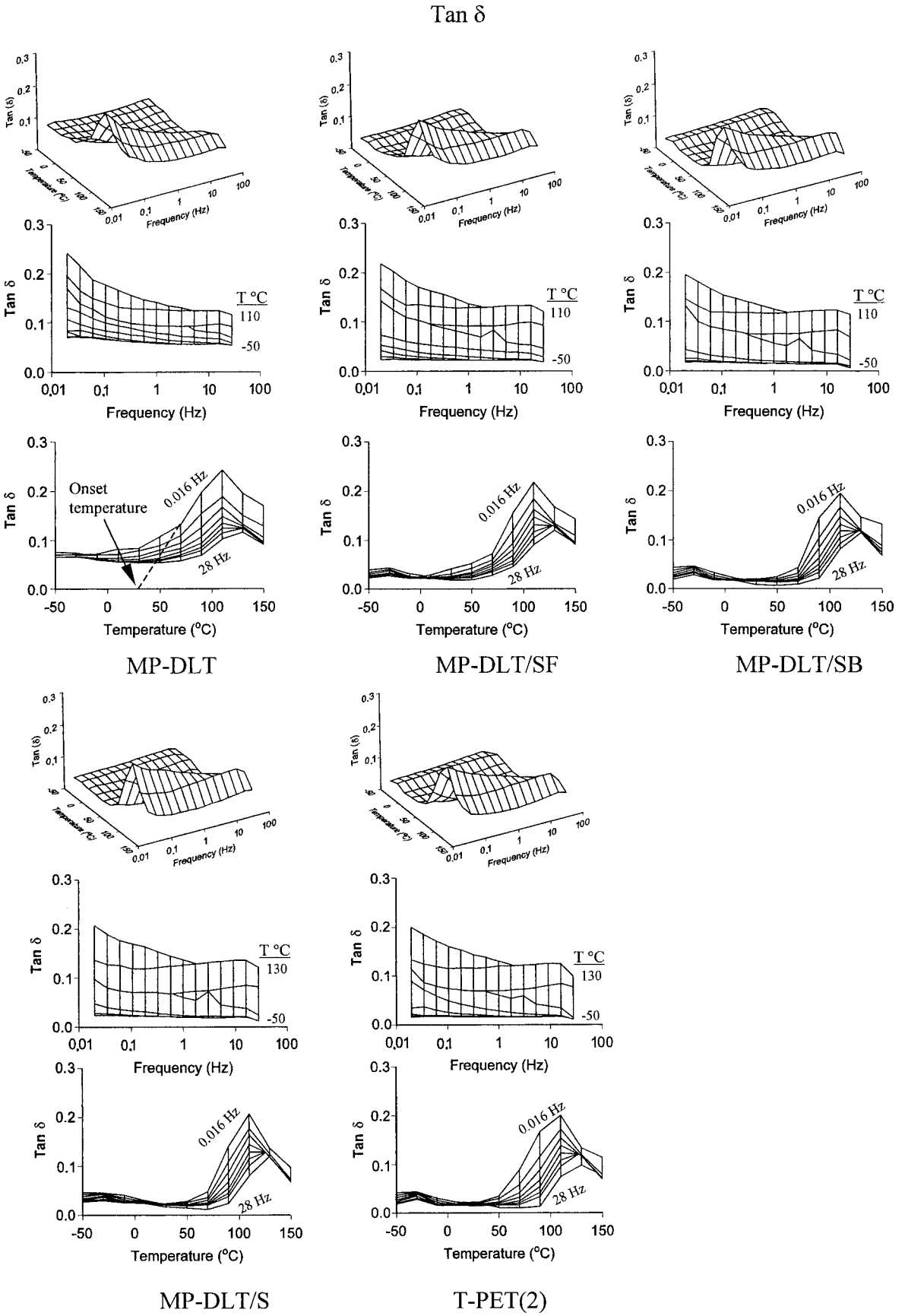

Figure 8 (*Continued from the previous page*)

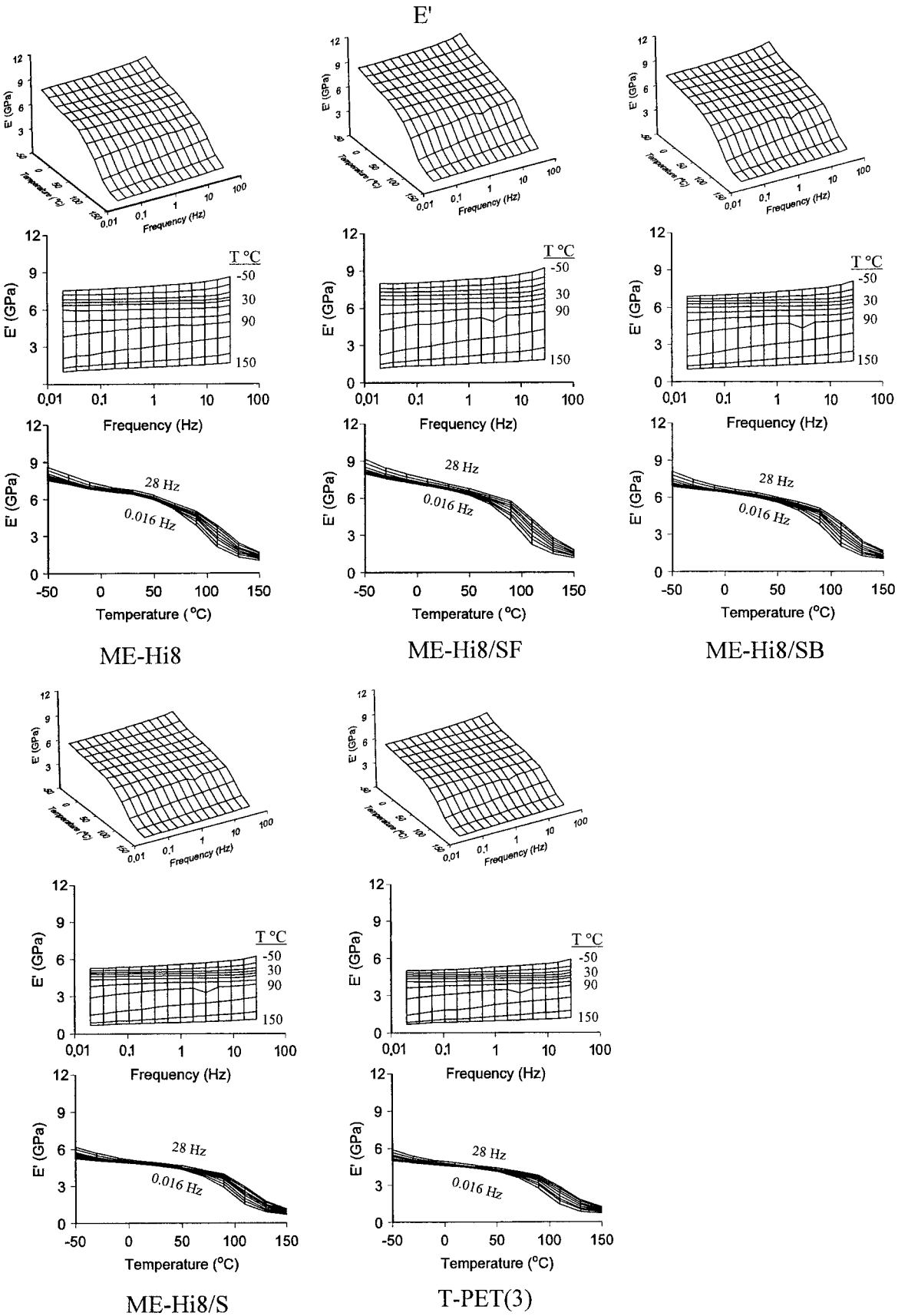

Figure 8 (*Continued from the previous page*)

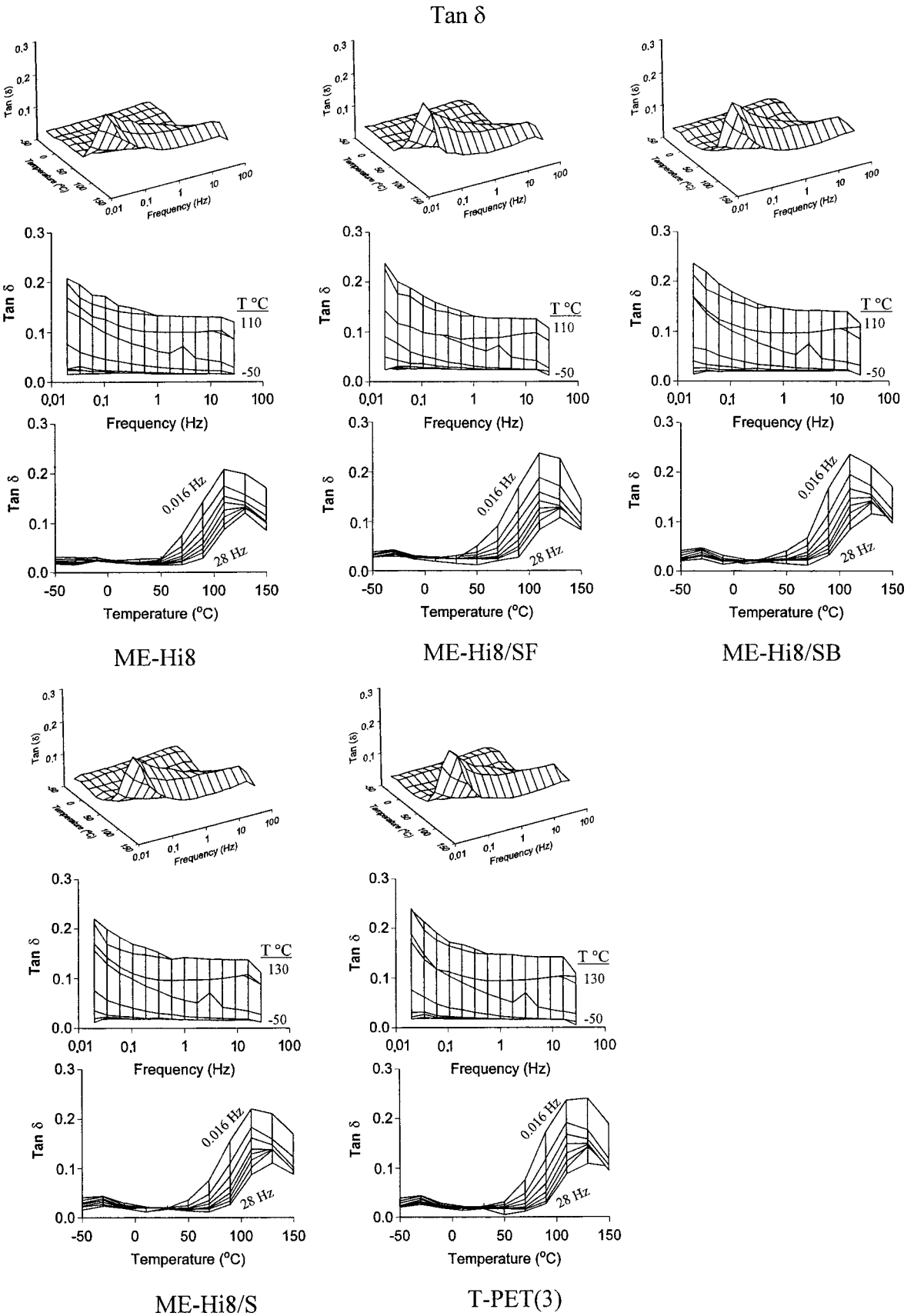

Figure 8 (*Continued from the previous page*)

TABLE II
Summary of Properties for Various Samples in MD

Sample	CTE ($\times 10^{-6}$/°C) at 25–35% RH (30–40°C)	CHE ($\times 10^{-6}$/% RH) at 25°C (15–80% RH)	E' (GPa) at 25°C, 45–55% RH		Poisson's ratio[a,b]	Longitudinal elongation[a] (%)		Lateral contraction[a] (%)	
			0.016 Hz	28 Hz		12 min	50 h	12 min	50 h
MP-DLT	3.8	10.9	7.2	8.2	0.24	0.099	0.105	0.027	0.031
MP-DLT/F	9.9		10.3	12.0					
MP-DLT/B	12.0		12.6	15.0					
MP-DLT/S	−2.6		7.3	7.9	0.34	0.118	0.124	0.036	0.040
T-PET(2)	−4.5	13.0	7.1	7.5	0.32	0.100	0.113	0.033	0.034
MP-LTO	1.8	10.7	7.1	9.1	0.29	0.109	0.123	0.037	0.041
MP-LTO/S	−3.5		6.5	8.6	0.37	0.130	0.144	0.045	0.052
T-PEN	−6.3	10.6	6.6	9.0	0.38	0.136	0.158	0.047	0.055
ME-Hi8	9.9	6.6	6.4	6.8	0.20	0.148	0.163	0.028	0.029
ME-Hi8/F	7.1		140	153					
ME-Hi8/B	15.3		46	49					
ME-Hi8/S	13.5		4.7	4.9	0.21	0.172	0.177	0.042	0.044
T-PET(3)	14.3	8.9	4.4	4.7	0.21	0.167	0.173	0.035	0.038
ME-MDV	9.9	6.9	6.3	7.6	0.20	0.114	0.132	0.024	0.025
ME-MDV/S	12.3		5.2	6.7	0.19	0.168	0.190	0.035	0.042
T-PEN(2)	12.4	3.0	4.6	5.9	0.23	0.191	0.195	0.039	0.044

[a] Test condition: 25°C, 50% RH.
[b] Measured at a stress range from 5 to 40 MPa, stress step of 7 MPa, and time interval of 12 min.

responding data for the ME-Hi8 tape and substrate were 6.9 and 4.9 GPa, respectively. The differences in the moduli of the tapes primarily originate from differences in the moduli of substrates. The selection of the substrate is determined by the tape application. The MP tapes in this study were used in linear drives, whereas the ME tapes were used in rotary drives. In the case of linear drives, high elastic modulus along the longitudinal direction is required for thinner substrates to avoid stretching. In the case of rotary drives, the track is written along an axis at an angle, on the order of 5°, to the tape length. The lateral deformation is more important than the longitudinal direction of the tape in the rotary drive system, given that the tension in the lateral direction is higher than that in the longitudinal direction. Thus the substrates for ME tapes are generally "balance" drawn or slightly tensilized along the transverse direction (TD), not like the substrates for MP tapes that are highly tensilized in MD.

As a summary, the dynamic mechanical property of magnetic tape is governed by its substrate material. MP tapes show slightly greater viscoelastic behavior than that of their substrates, whereas there are no obvious differences between the viscoelastic behavior of ME tapes and their substrates. The PEN-based tapes have good elastic stiffness at high frequency and low temperature, whereas the PET-based tapes have low loss tangents and stable moduli below the T_g temperature. The substrates for MP tapes were selected to have high moduli along the longitudinal direction, whereas this is not the top priority for the substrate for ME tapes.

Master curves of storage modulus

Based on the storage modulus data in Figure 8, master curves of storage moduli for finished tapes, substrates, and virgin films (storage moduli data for MP-LTO and ME-MDV are not included) were generated by applying the technique known as frequency–temperature superposition.[15,18] Using this technique, storage moduli measured at the elevated temperatures are superimposed to predict the behavior at longer time periods (lower frequencies) at a reference temperature of 30°C. The results are presented in Figure 9. The technique gives a wide perspective on the storage moduli for the tape and substrates. Also, we can have a clear comparison between the substrates and the virgin films, and see the effects of the tape manufacturing process on the storage moduli of substrates.

Calculation of mechanical properties of individual layers

Applying the rule of mixtures [eq. (12)] to the data of substrate and combined layers (substrate plus front coat or substrate plus back coat), the mechanical properties of the individual layers, say front coat or back coat, can be calculated. The calculated storage moduli for individual layers are plotted in Figure 9. The figure shows the calculated storage moduli for front coat and back coat. Both the front and back coats in MP-DLT tape have higher storage moduli than that of the substrate. The back coat shows constant modulus over a wide frequency range, which is not seen for other

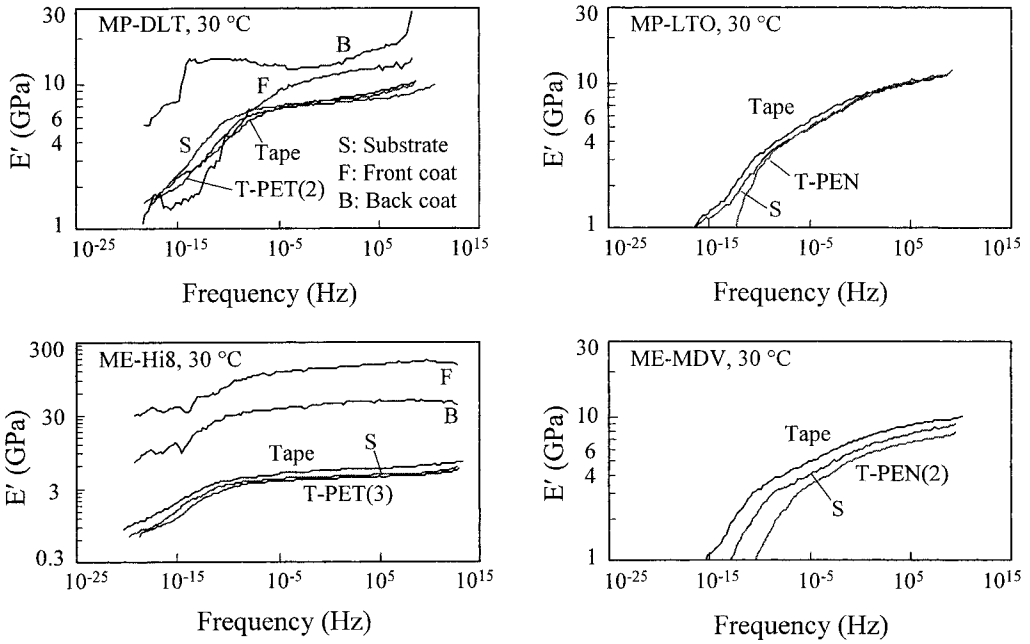

Figure 9 Master curves of storage moduli for various samples and corresponding layers.

materials in this study. The abnormally high values around 10^{-15} Hz for the back coat may come from the measurement error. The behavior of the substrate at this frequency is comparable to its behavior at the temperature around T_g. The increased deformability of the substrate may affect the accurate DMA measurement on the combined layers. The calculation results for ME-Hi8 samples show that the front coat has a significantly higher storage modulus, on the order of 100–200 GPa. It is reasonable that the front coat has a much higher storage modulus than that of the substrate because the front coat contains DLC, which is supposed to have extremely high stiffness.

It will be shown later that for calculation of CTE for the individual layers, we would need complex moduli for the various samples. Trends for the complex modulus are expected to be similar to those for the storage modulus.

Effect of the tape manufacturing processing on the DMA of substrate films

From DMA results, based on Figure 9 and Table II, it is interesting to note that for all four tapes, none of the substrates showed degradation compared to the virgin film; instead, most of substrates showed strengthened storage moduli after manufacturing. Studies have shown that the annealing of the polyester film under T_g does not result in a significant decrease in mechanical properties,[1,19,20] whereas Gillmor and Greener[21] found that annealing treatment on PEN films resulted in lower loss tangent at the α-relaxation, and a lower decrease in relaxation moduli (moduli at very low deformation frequencies).

All the substrate films used in this study were biaxially oriented, and were metastable in two respects. First, the percentage crystallinity of the film was much lower than the equilibrium crystallinity content. When the temperature was high, the molecular segments in amorphous region tended to move and form oriented chains or even crystallize to reduce the system entropy. High crystallinity resulted in high mechanical properties. Second, amorphous regions of the film contained a frozen-in strain, which tended to relax and cause the film to contract.[1] Annealing under T_g, which occurs during the tape manufacturing, helps to thermal-set the film and increase the dimensional stability.

On the other hand, when the temperature is higher than the glass-transition temperature, the main chain of the polymer film molecules will have enough energy to move and rotate. As a result, the biaxially oriented structure could be significantly affected. The mechanisms of thermal degradation include the residual stress relaxation, recoiling of molecule segments, and selected-chain scission or random-chain scission.[22] Stress relaxation also reduces the anisotropy of the film's mechanical properties. This effect is, obviously, more significant for the films that are highly tensilized in one direction, say MD. Because the MP-DLT and MP-LTO tapes are used for linear drives, the substrates T-PET(2) and T-PEN are more stretched in MD than in TD. The effect of strengthening and weakening of the MP tape manufacturing process thus seems to counteract the stress relaxation effect, and

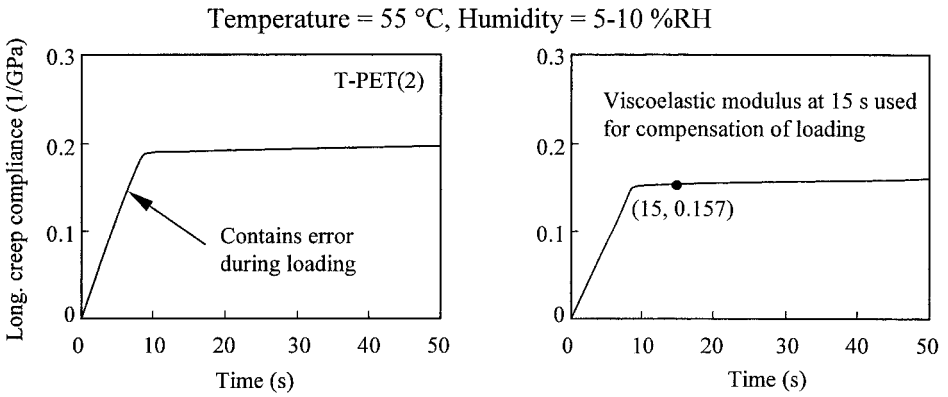

Figure 10 Schematic diagrams of "toe" compensation: (a) raw data from short-term creep test, (b) compensation of loading for T-PET(2) film.

there is almost no change to the storage moduli between the substrates and the virgin films. In the case of ME tapes, the balance-drawn films were less affected by the residual stress relaxation than those tensilized films used for MP tapes. Thus, both the ME tape substrates show strengthening compared to the virgin films. The reason that the T-PEN(2) film shows greater strengthening than T-PET(3) film comes from the fact that PEN films contain a more extensive amorphous region, and have a larger driving force for stress relaxation and recrystallization at elevated temperature, than PET films.

Long-term longitudinal creep tests

Calibration and compensation of the experimental deformation at 7 MPa

During the longitudinal deformation tests, the strain in 7 MPa stress range at the initial loading duration was not stable, which covered the so-called toe region in the engineering strain–stress curve (ASTM 882-97[16]). According to ASTM standards, the deformation of the sample in the low-stress range, either loading or unloading, contains an artifact that is caused by a take-up of slack, and alignment or seating of the specimen, which does not represent a property of the material (Fig. 10, left curve). To give quantitative demonstration, we first define a term, viscoelastic modulus, as the stress amplitude divided by the strain amplitude over a period of loading. The period should avoid the unstable loading zone. In this study, 15 s was chosen. The viscoelastic modulus represents the combination of elastic and viscoelastic properties of the films. Although the moduli should be a stable value for linear viscoelastic samples, stable experimental moduli are obtained only when the stress is higher than a certain value ("toe" stress value). Very careful sample mounting may reduce this value. Because of the existence of the toe stress, when a load is applied on the sample, the real stress in the sample deviates from the calculated value, although the deviation amplitude is uncertain. However, throughout the test period, the deviation amplitude is a constant. That is, the experimental creep compliance curve shifts a constant value from the expected curve attributed to the toe stress.

To remove the effects of toe region, compensation was made by applying the stable viscoelastic modulus to calculate the theoretical initial strain and creep compliance at a 7 MPa stress span. To obtain the theoretical initial strain at a 7 MPa stress, tests were performed on a sample identical with the creep test sample. The test conditions (temperature, humidity, and conditioning time) should be the same as those of the creep test. The tests were performed using the following steps.

After conditioning without preload for 1 h and then with 0.5 MPa load for an additional 2 h, the sample was preloaded at 5 MPa for 0.5 h at corresponding temperature and humidity. Then an extra 7 MPa load was applied and the strain at 15 s was recorded. The viscoelastic modulus of this sample at 15 s, corresponding to a preload stress of 5 MPa, was calculated from dividing the applied stress of 7 MPa by the strain increment after the 7 MPa load. The load on the sample was removed and the sample was allowed to have a short recovery period (about 5 min). A 10 MPa load was applied on the tape for 0.5 h, after which an extra 7 MPa was added. Again the strain at 15 s was measured and was used to calculate the viscoelastic modulus of this sample at a preload stress of 10 MPa. This process was continued at elevated load up to 25 MPa. Thus five values of the viscoelastic moduli as a function of stress were obtained. For the purpose of demonstration, viscoelastic moduli of samples from MP-DLT and ME-Hi8 are shown in Figure 11. The moduli at stable stress range were then averaged to obtain the final viscoelastic modulus for each film at each temperature.

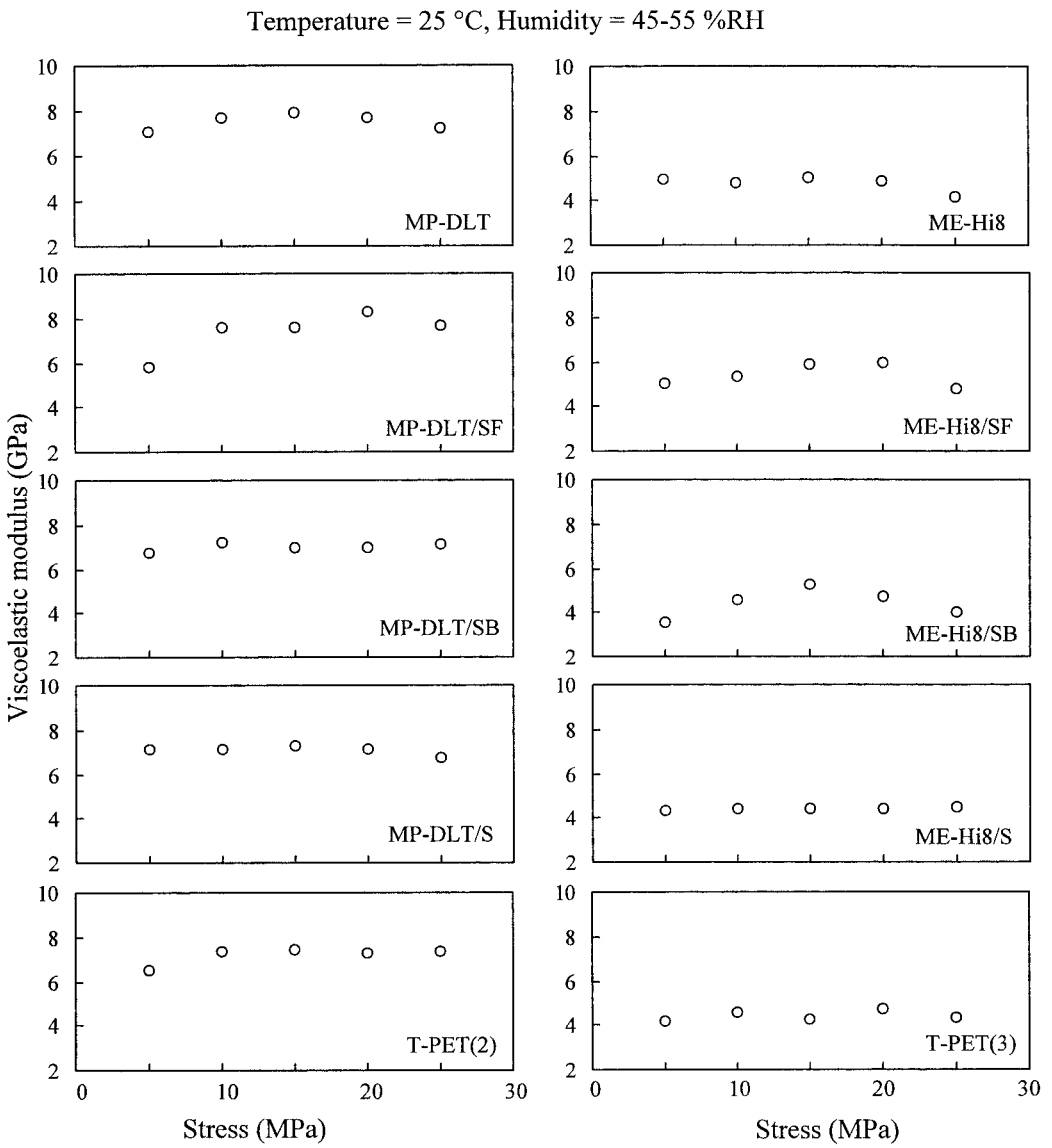

Figure 11 Viscoelastic moduli for MP-DLT and ME-Hi8 samples as a function of average stress at 25°C, 45–55% RH (loading period: 15 s).

The creep compliance compensation procedure is schematically illustrated for T-PET(2) film in Figure 10 (right curve). The compensation was achieved by shifting the original creep compliance curve (left curve) to the value at 15 s, which was obtained by taking the inverse of the viscoelastic modulus value. In the example shown, the creep compliance of T-PET(2) film at 15 s is 0.157 GPa^{-1} for viscoelastic modulus value of 6.37 GPa.

Long-term creep behavior

Creep compliance as a function of time for various samples at 25°C/50% RH, 40°C/25% RH, and 55°C/10% RH are shown in Figure 12(a)–(c). Both linear scale and log–log scale plots are presented in the figure. Compared to linear scale plots, which give general information during the whole 50-h period, log–log scale plots provide more detailed information on the initial creep period. The values of creep compliance at 50 h are also listed in Table II.

From the creep compliance of MP-DLT shown in Figure 12, it is found that the trends of creep between different samples are similar at 25 and 40°C. That is, the substrate has the highest creep, which is followed by SB composite. The SF composite has the lowest creep. The creep value of the tape is between that of the SB composite and that of the SF composite. At 55°C, however, the creep compliances of the substrate and SB composite decrease with time after the initial elongation, and the substrate exhibits the lowest creep. At the same time, creep compliances of the tape and

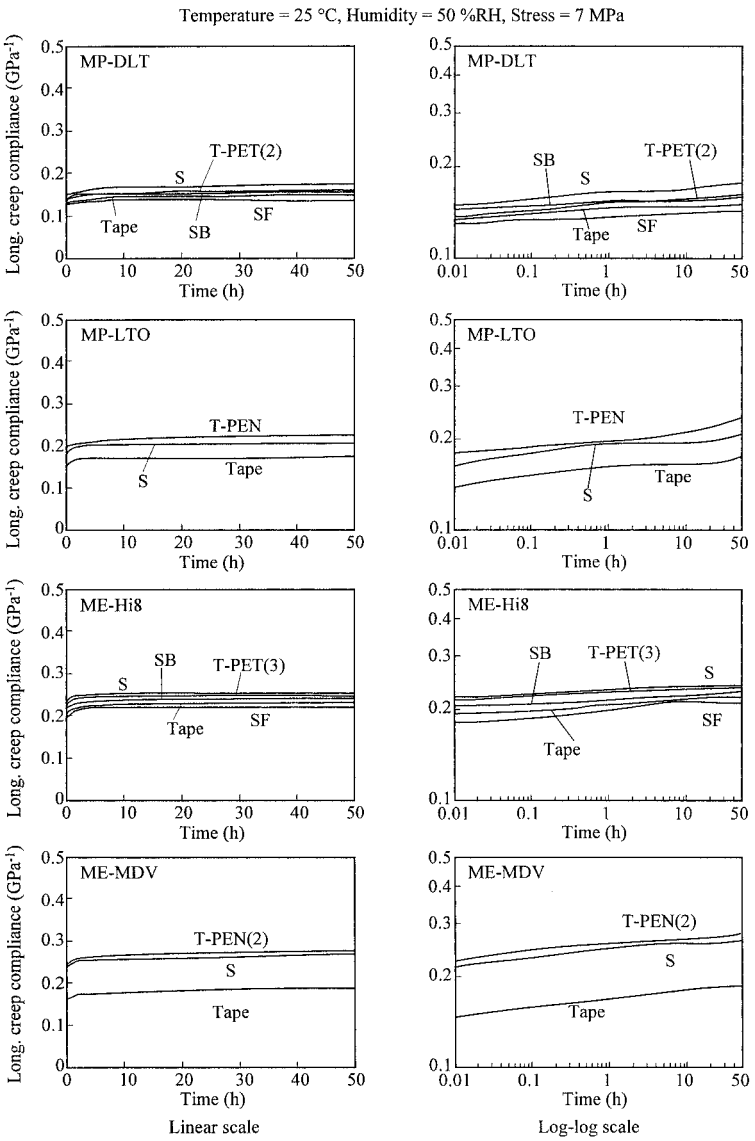

Figure 12 Creep compliance measurements for various tape samples at (a) 25°C, (b) 40°C, (c) 55°C, plotted on linear scale, and logarithmic scale.

SF composite continue to increase with time. For ME-Hi8, the creep of the SB composite is lower than that of the substrate but higher than that of the tape and SF composite. The SF composite maintains the lowest creep at all test temperatures. For MP-LTO and ME-MDV, a stable relationship of creep between samples is maintained at all test temperatures; that is, substrates always have higher creep than that of the other composites.

By comparing the creep of virgin polymeric film with that of the substrates from the tape, it was found that T-PET films have lower creep than that of corresponding substrates, whereas PEN films have higher creep than that of the tape substrates. The change is attributed to the manufacturing process and the nature of the films. The only exception is T-PET(2) and corresponding substrate from the tape at 55°C. The creep compliance of T-PET(2) almost remains constant over the test period after the initial elongation. This means that both creep and shrinkage occur simultaneously and the film maintains an equilibrium condition at 55°C. The shrinkage is caused from the relaxation of residual stress in the highly tensilized material. The corresponding substrate, however, exhibited apparent shrinkage after the initial deformation, which shows that the relaxation of residual stress in T-PET(2) is accelerated after the tape manufacturing.

MP tapes (MP-DLT and MP-LTO) show better dimensional stability than that of ME tapes (ME-Hi8 and ME-MDV) at lower temperature. In particular, MP-DLT maintains good stability at all test temperatures. As discussed in DMA test results, MP-DLT and MP-LTO are used in linear drives. The linear drive requires the tapes to avoid stretching in the machine

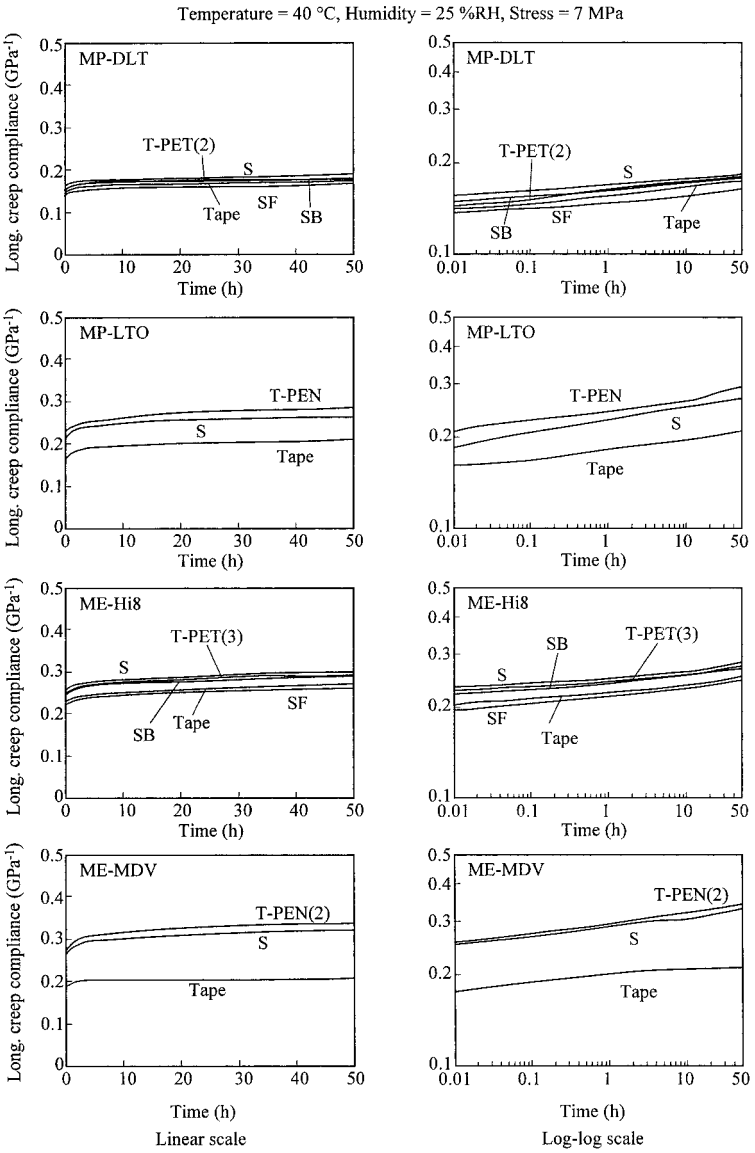

Figure 12 (*Continued from the previous page*)

direction under operating tension. For this reason, the substrates for MP-DLT and MP-LTO are highly tensilized in the machine direction.

Master curves of creep compliance

Using the time–temperature superposition technique,[15,18] master curves of creep compliance for all tested samples [see Fig. 13(a)] were generated from the test results in Figure 12. A reference temperature of 25°C was taken, and the creep compliances at 40 and 55°C were shifted to generate long-term creep compliance up to 10^8 h.

Calculation of creep compliance of individual layers

The creep compliances of front coat and back coat were calculated from the creep test results of the composite and the substrate using the rule of mixtures for MP-DLT and ME-Hi8. The results are shown in Figure 13(b). From the figure, both front coat and back coat of MP-DLT have lower creep than the substrate before 10^6 h. After that, the substrate shrinks, whereas the front coat and back coat continue to elongate. The creep of each individual layer of ME-Hi8 increases monotonically with time. The front coat of ME-Hi8 is found to have much lower creep than that of the substrate and the back coat. This trend corresponds to the extremely high storage modulus of the front coat calculated from the DMA test results. To show the correctness of the rule of mixtures, the creep compliance of the finished tape for MP-DLT and ME-Hi8 was calculated and compared with the experimental value. The comparison is shown in Figure 13(c). A good match between the calculated result and experimental value was obtained.

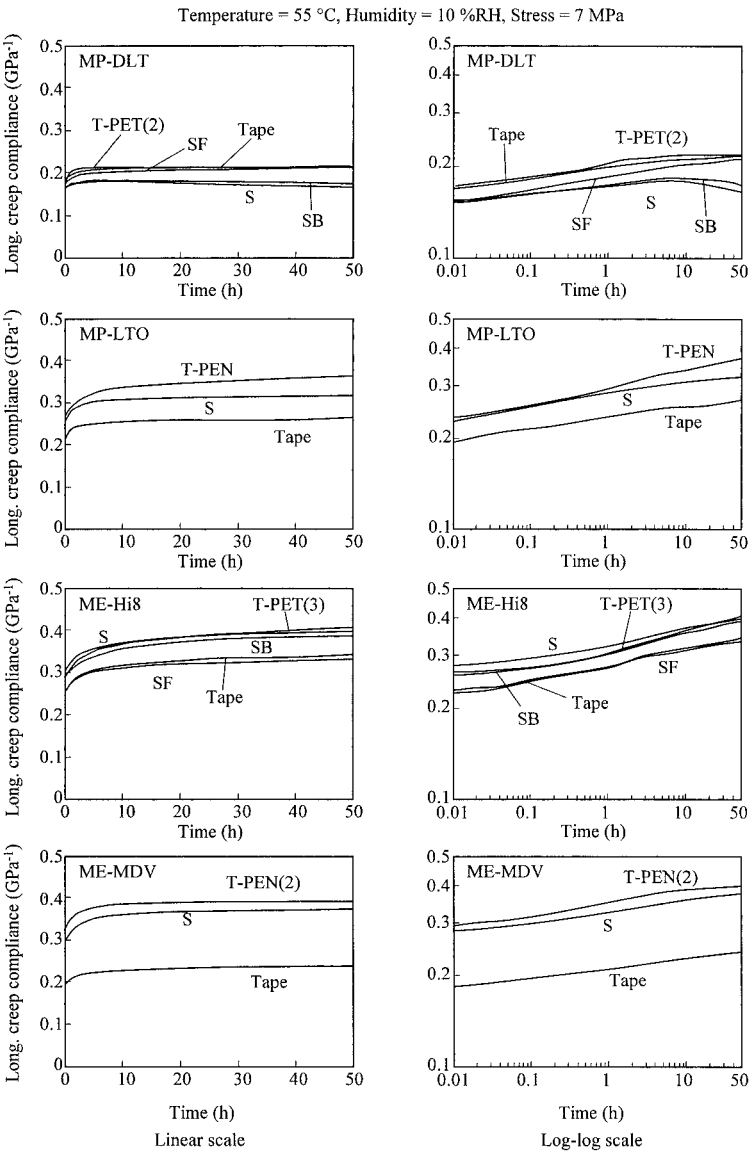

Figure 12 (*Continued from the previous page*)

Effect of tape manufacturing processing on the longitudinal creep compliance of substrate films

It was found that PET films degraded after manufacturing, whereas PEN films were enhanced by the processing [except for T-PET(2) at 55°C where shrinkage occurred on the substrate from the tape]. The trends in change of PEN films after manufacturing are the same as those in DMA test results. However, the effect of manufacturing on creep of PET films is different from that by DMA of PET films. The reason lies in the difference of T_g between PET films and PEN films. The T_g of PEN films is about 120°C, whereas the T_g of PET films is about 80°C. During the manufacturing of MP tapes, the tape is processed at 50–80°C.[1] The temperature is far lower than the T_g of PEN films, although very close to the T_g of PET films. The manufacturing processes help to thermal-set the tensilized PEN film. As a result, PEN films become more stable after manufacturing. The manufacturing temperature is so close to T_g of PET film that the properties of PET films could be slightly influenced. Consequently, in the creep test the substrates from tape are degraded.

The temperature is higher in ME tape manufacturing than that in MP tape processing, which may be closer to the T_g of PEN. However, the manufacturing process confers the same effect on the substrates as in the case of the MP tapes.

Effect of temperature on the longitudinal creep compliance

To show the relationship between the creep compliance and the temperature, temperature-dependent creep compliance at 50 h is presented in Figure 14. The

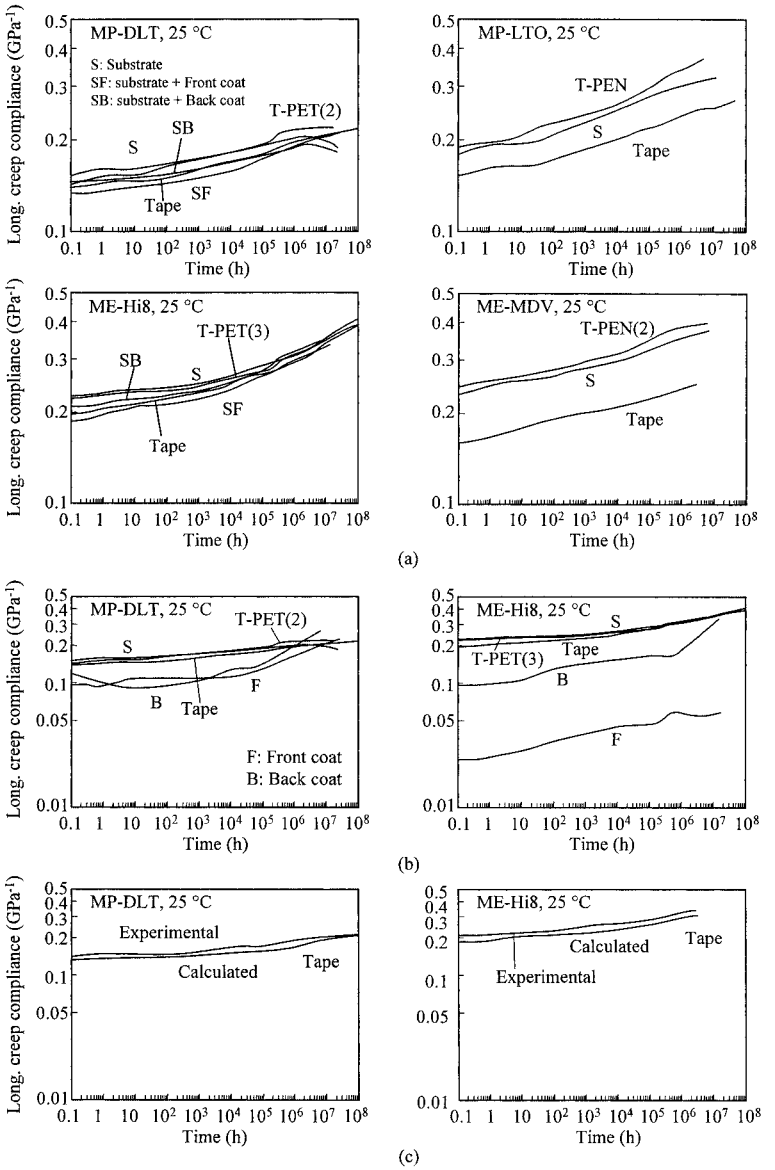

Figure 13 (a) Creep compliance master curves for all tested samples at 25°C. (b) Creep compliance master curves at 25°C of front coat and back coat for MP-DLT and ME-Hi8 from calculation, compared with the tape, the substrate, and the virgin film. (c) Comparison of experimental and calculated creep compliance for finished tapes.

plots in the figure show a linearity of MP-LTO and ME-MDV. The tape and SF of MP-DLT and the tape and SF of ME-Hi8 also show good linearity. The creep compliances of substrate and SB of MP-DLT decrease at high temperature. The substrate and SB of ME-Hi8, on the contrary, exhibited a larger creep ratio than that of tape and SF, and also larger than that of other films.

Poisson's ratio and lateral creep

Poisson's ratio

The Poisson's ratio data for various samples are summarized in Table II.[11] It should be noted that the "Poisson's ratio" is the average value over a stress range of 5 to 42 MPa, whereas the "lateral contraction" and "longitudinal elongation" also presented in the table were obtained at 7 MPa. Thus the Poisson's ratio in the table may not be exactly equal to the ratio of lateral contraction over longitudinal elongation in that table.

Generally, ME tapes show lower lateral contraction and lower Poisson's ratio than those of MP tapes.

It is interesting to note that the substrates for ME tapes have low Poisson's ratios, and are very close to the Poisson's ratio of the final tape. Tape manufacturers probably selected the substrate so that there is less

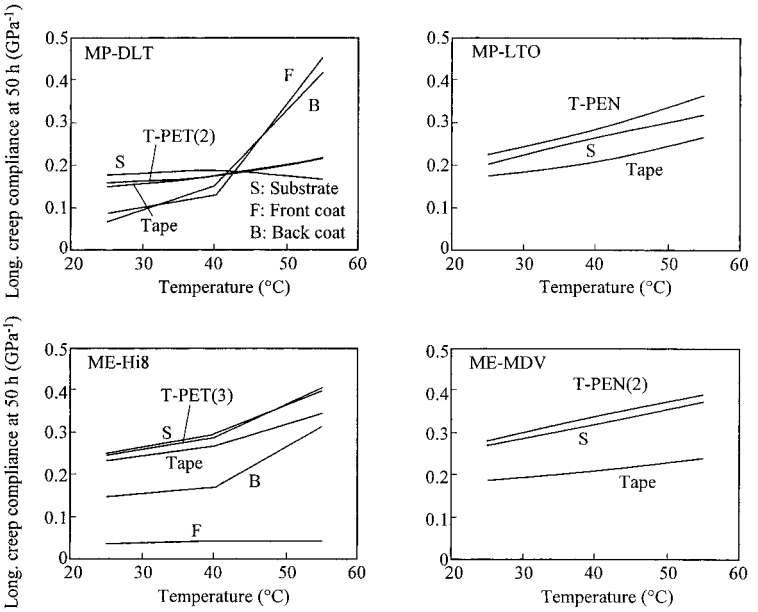

Figure 14 Temperature dependency of the creep compliance at 7 MPa stress, and 50 h.

strain mismatch between the substrate and ME front coats.

Lateral creep

Figure 15 shows the lateral creep of the various layers of the tapes, on both a linear scale and a log–log scale.[11] Based on the data of the substrate and combined layers (SF and SB), a model was developed by Ma and Bhushan[11] to calculate the lateral creep of the individual layers of the magnetic tapes. Unfortunately, we need Young's moduli data for the tape samples (including combined layers SF and SB) in TD, and they were not available in this study because of the sample size. Theoretically, these moduli can be obtained from the tape web before it is slit.

Next we examine the effect of tape manufacturing processing on the lateral creep. From the creep test results, it was found that both T-PET(2) and T-PET(3) showed slight degradation from the raw film to the stripped substrates of tapes. Moreover, the T-PEN and T-PEN(2) showed enhancement after the manufacturing. The change in lateral creep after manufacturing corresponds well to the longitudinal creep.

Hygroscopic expansion and thermal expansion

Hygroscopic expansion

CHE is another important factor in magnetic media and other applications.[1,23] After all, the environmental relative humidity changes as dramatically as, if not more than, the temperature does. Table II summarizes the data for various samples.[11] The error of CHE was estimated to be within $\pm 0.5 \times 10^{-6}$/% RH. The CHE values for MP tapes and substrates were found to be higher than those for ME tapes and substrates.

Applying the rule of mixtures one may also obtain the CHE for the individual layers of magnetic tapes, although it requires the moduli of the sample at various relative humidities, and requires further work.

Thermal expansion

The CTE data measured by TMA are plotted in Figure 16 and also summarized in Table II.[11] By applying the rule of mixtures, CTE of individual layers can be calculated from the data of combined layers. For the original unit length combined layer structure ($x_0 = 1$), after a unit temperature increase ($\Delta T = 1$), the structure expands by Δx_{sf}. Assuming that the thermal expansion of the tape samples along MD and TD are independent, the dimension and stress condition in TD are not considered in this work. If there were not interfacial bonding, the free thermal expansion of the substrate after the temperature increase would be Δx_s, whereas that of the front layer would be Δx_f. Thus, there shall be an interfacial shear stress that causes $(\Delta x_{sf} - \Delta x_s)$ deformation in the substrate and $(\Delta x_{sf} - \Delta x_f)$ deformation in the front layer; that is,

$$\sigma = (\Delta x_{sf} - \Delta x_f)E_f f = -(\Delta x_{xf} - \Delta x_s)E_s s \qquad (15)$$

Given that $\Delta x_s = \alpha_s x_0 \Delta T$, we have

$$E_f f(\alpha_{sf} - \alpha_f) = E_s s(\alpha_s - \alpha_{sf}) \qquad (16)$$

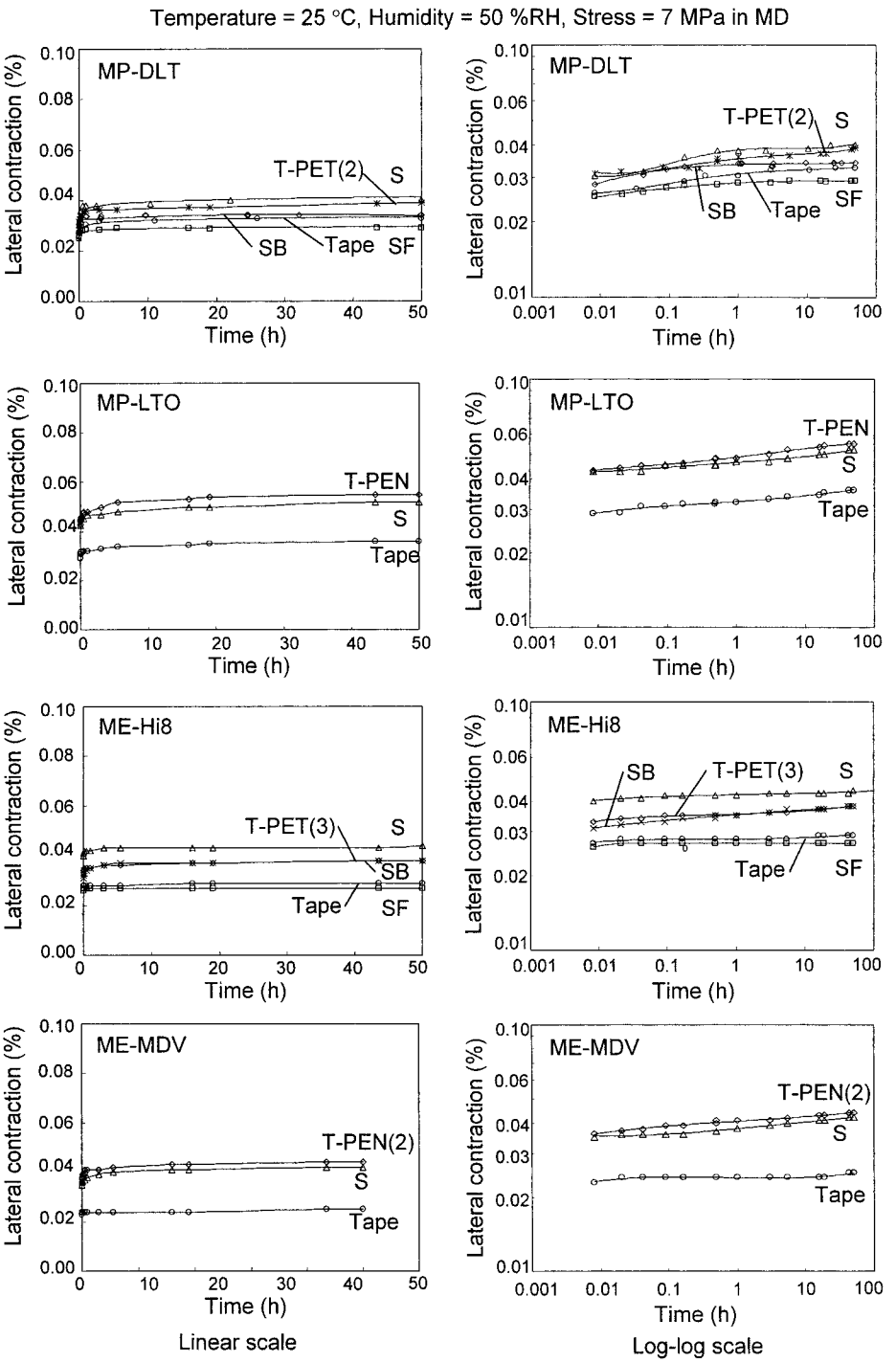

Figure 15 Lateral creep of tapes and tapes with some of the layers removed.

where α_s, α_f, and α_{sf} are the CTE values of the substrate, front coat, and the composite, respectively. So we have

$$(E_f f + E_s s)\alpha_{sf} = E_f f\alpha_f + E_s s\alpha_s \tag{17}$$

By considering eq. (12), we finally obtain

$$E_{sf}(f + s)\alpha_{sf} = E_f f\alpha_f + E_s s\alpha_s \tag{18}$$

In the case that E_{sf}, f, s, α_{sf}, E_f, α_f, E_s, and α_s are known, we can calculate α_f, the CTE of the front coat layer, and, similarly, the CTE of the back coat.

The rule of mixtures is based on an "isostrain" assumption. For a composite during thermal expansion, the strain includes both elastic and viscoelastic

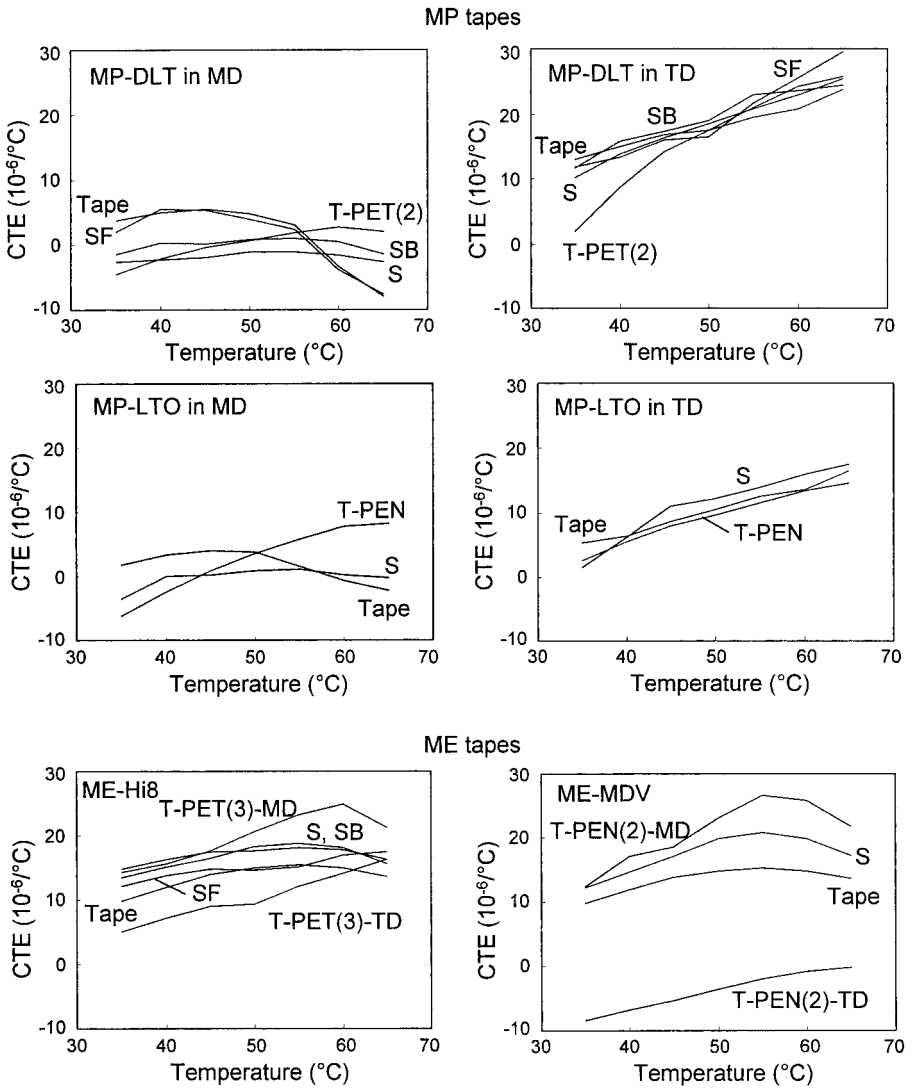

Figure 16 Coefficient of thermal expansion as a function of temperature for various samples.

parts. Thus the complex modulus, instead of storage modulus, was used in the rule of mixtures calculations of CTE for the individual layers. The complex moduli can be calculated from the test at 0.016 Hz and 30, 50, and 70°C. The CTE values of front and back coats of MP-DLT and ME-Hi8 are calculated and listed in Table II. The data are on the same order as those of the substrate, whereas the CTE for front coats is lower than that for back coats, for both MP and ME tapes. In MP-DLT samples, the CTE of the substrate is negative all through the 30 to 70°C temperature range, showing that T-PET(3) has a large residual stress that continues to relax during the heating. The CTE for the front coat shows a sudden shrinkage at high temperature (60–70°C). Considering the stable data of the substrate and back coat, it is reasonable to believe that the shrinkage of the tape at 60–70°C is contributed by the front coat. In the ME-Hi8 sample, all the layers and the tape show constant positive CTE through the testing temperature range, which indicates that the residual stress along the MD does not exist in any layers of this tape.

Summary of the properties for tape samples

Mechanical properties

Figure 17(a) summarizes the storage moduli of various samples at 0.016 and 28 Hz at 25°C, where the data are linearly interpolated from the storage moduli data at 10 and 30°C from DMA testing. Other relevant mechanical properties, the Poisson's ratio, longitudinal elongation and lateral contraction for the various samples are shown in Figure 17(b)–(d). In Figure 17(a) and (b), tapes show similar properties with their substrates. The storage moduli for PEN-based tape, MP-LTO and ME-MDV, increase significantly as the deformation frequency increases, which are identical to the storage moduli as a function of deformation fre-

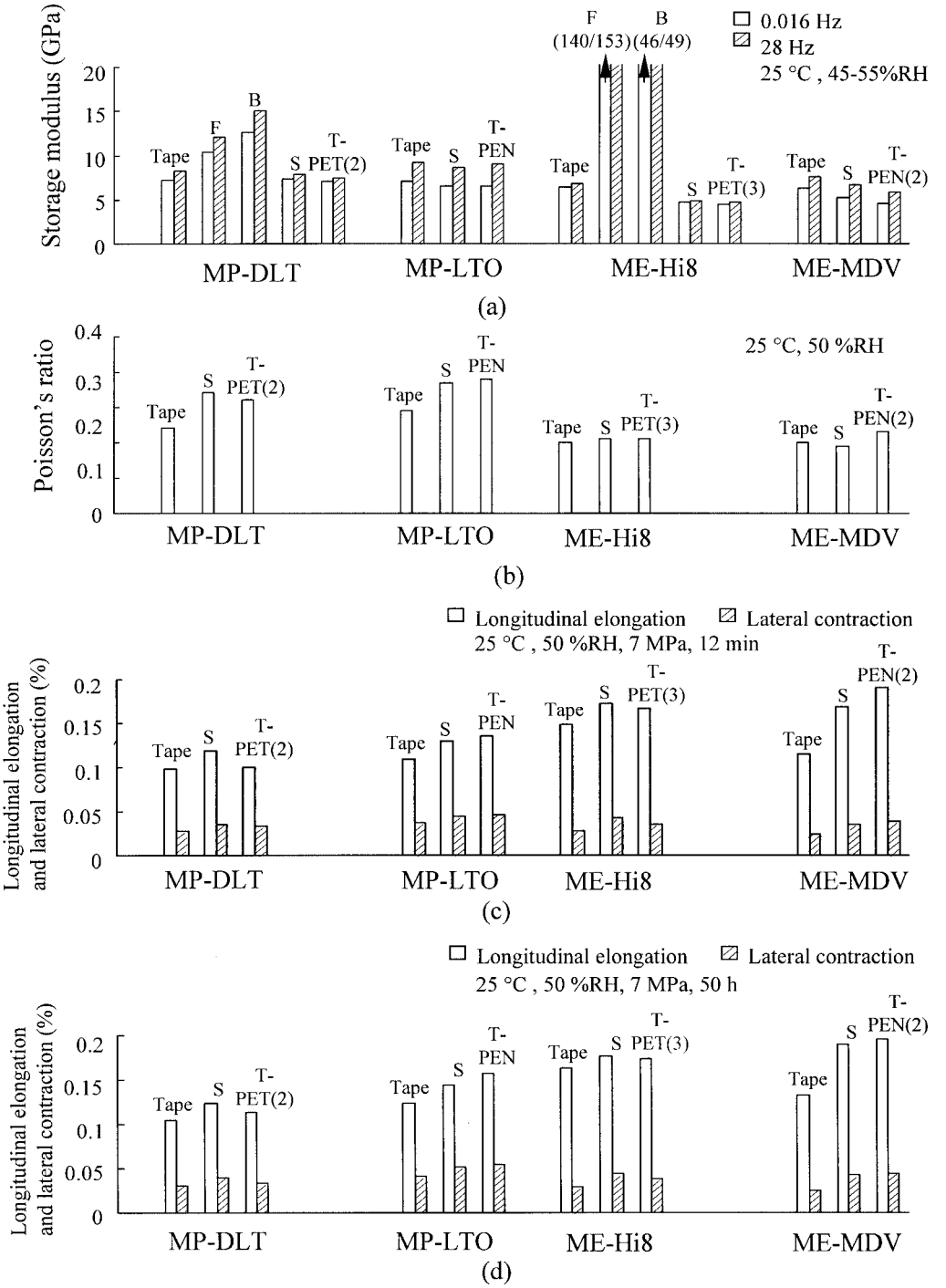

Figure 17 Summary of the elastic and viscoelastic properties for various samples. (a) Storage moduli: data for the front and back coats are calculated; all the others are measured. The reproducibility for DMA measurement is about ±5%. (b) Poisson's ratio; the error is about ±5%.[9,11] (c) Longitudinal elongation (this study) and lateral contraction[11] for various samples at 25°C, 50% RH, 7 MPa uniaxial stress for 30 s and 12 min, respectively. The reproducibility for the measurement is about ±5%. (d) Longitudinal elongation (this study) and lateral contraction at 25°C, 50% RH, 7 MPa uniaxial stress for 50 h.[11]

quency for PEN substrates in this work and in a previous DMA study.[8] The Poisson's ratio for the ME tapes, ME-Hi8 and ME-MDV, was found to be around 0.20, very close to that for the corresponding substrates, T-PET(3) and T-PEN(2). Poisson's ratios for MP tapes were slightly lower than those for their substrates. The viscoelastic properties in Figure 17(c) are slightly different from the elastic properties in Figure 17(a). The MP-DLT/S and ME-Hi8/S show slightly weakened viscoelastic properties compared to those of the virgin films, whereas there is either no change or a slight strengthening in elastic moduli.

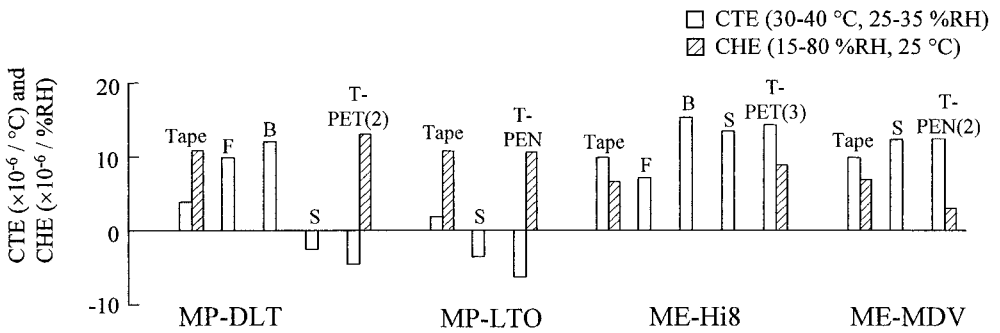

Figure 18 Summary of the CTE and CHE for various samples. The error for CTE is about $\pm 1.5 \times 10^{-6}$/°C, and the error for CHE is about 0.5×10^{-6}/% RH.

However, the MP-LTO/S and ME-MDV/S show obvious strengthening compared to that of PEN films. The lateral creep data in Figure 17(d) show results similar to those in Figure 17(c); generally, ME tapes exhibit less lateral contraction than the MP tapes do, at current test conditions.

Hygroscopic expansion and thermal expansion

The CHE and CTE for various samples are summarized in Figure 18. It is clear that the properties of magnetic tapes are governed by their substrates. MP tapes use highly tensilized substrates, which have negative CTE, and as a result, the CTE values for MP tapes are significantly lower than those for ME tapes, which use balance-drawn substrates. The CHE values for MP tapes and substrates were found to be higher than those for ME tapes and substrates.

CONCLUSIONS

The mechanical properties of magnetic tapes are generally governed by their substrate materials. The storage moduli for MP tapes and substrates are higher than those for ME tapes and substrates along the longitudinal direction; this is because the substrates are selected according to the requirement for the linear and helical drive systems, in which the MP and ME tapes are used.

With respect to the effect of tape manufacturing process, the storage moduli for the substrates of ME tapes are higher than those for the virgin films. This is believed to be attributable to the thermal-setting effect of the tape manufacturing process. T-PEN(2) film shows greater strengthening than T-PET(3) film after ME tape manufacturing because PEN film contains a more extensive amorphous region and is affected to a greater degree by thermal setting than the PET film.

The storage moduli of the front and back coats of MP and ME tapes were calculated by the rule of mixtures. Both the front and back coats for MP-DLT tape were found to be slightly stiffer than their substrates. Frequency–temperature superposition was used to obtain the data at a wide range of frequencies. The back coat was found to have a constant modulus over a wide frequency range from 10^{-10} to 10^{10} Hz. The modulus for the front coat for ME-Hi8 was found at the order of 100–200 GPa, and the modulus for the back coat was also higher than that for the substrate.

The Poisson's ratios for MP-DLT and MP-LTO were 0.24 and 0.29, respectively, whereas the ratio for both the ME-Hi8 and ME-MDV was 0.20. The Poisson's ratios for substrate films in this study ranged from 0.21 to 0.38.

The results of longitudinal creep and lateral creep showed that, at 25 and 40°C, all tested substrates have higher creep than that of corresponding finished tapes. At 55°C, the substrate of MP-DLT shrank and exhibited the lowest creep. Meanwhile, all other tested substrates maintained the highest creep. The PET films were degraded after either MP or ME tape manufacturing, whereas the PEN films were enhanced by the processing. The creep compliances of the front coat and back coat of both MP-DLT and ME-Hi8 were calculated. For MP-DLT, the substrate has larger creep than that of front coat and back coat before 10^6 h. After that, the substrate started to shrink, whereas the front coat and back coat continued to elongate. The creep compliance of substrate, front coat, and back coat of ME-Hi8 increased monotonically with time. The substrate of ME-Hi8 also had larger creep than that of other layers. The front coat of ME-Hi8 was found to have very low creep.

Based on the data of CTE and complex moduli of the tapes, substrates, and combined layers, the CTE values for the individual layers of the four tapes were calculated. The model provides a good match between the predicted CTE values for the finished tapes and the experimental data. The CTE for front coats for both MP-DLT and ME-Hi8 have lower CTE values than those for the corresponding back coats. The thermal shrinkage of the MP-DLT tape at 60–70°C is believed to be attributable to the shrinkage of the front coat at this temperature range. There was no thermal shrink-

age for the ME-Hi8 samples through the range of testing temperatures. The CHE for MP tapes samples was found to be higher than that for ME tapes samples.

The research reported in this paper was support by the industrial membership of Nanotribology Laboratory for Information Storage and MEMS/NEMS (NLIM) at The Ohio State University. The authors thank Hideaki Watanabe and Hirofumi Murooka from Teijin–DuPont Ltd. Japan; Toshifumi Osawa from DuPont–Teijin Ltd., for their generous support and samples [MP-DLT (Fuji), MP-LTO (IBM), ME-Hi8 (Sony), and ME-MiniDV (Panasonic)]; and Dr. Tiejun Ma for technical support and constructive discussions.

References

1. Bhushan, B. Mechanics and Reliability of Flexible Magnetic Media, 2nd ed.; Springer-Verlag: New York, 2000.
2. http://www.lto-technology.com/newsite/html/format.html.
3. Bhushan, B. Tribology and Mechanics of Magnetic Storage Devices, 2nd ed.; Springer-Verlag: New York, 1996.
4. Bobji, M.; Bhushan, B. J Mater Res 2001, 16, 844.
5. Weick, B. L.; Bhushan, B. J Info Storage Proc Syst 2000, 2, 207.
6. Weick, B. L.; Bhushan, B. J Appl Polym Sci 2001, 81, 1142.
7. Higashioji, T.; Bhushan, B. J Appl Polym Sci 2002, 84, 1477.
8. Bhushan, B.; Ma, T.; Higashioji, T. J Appl Polym Sci 2002, 83, 2225.
9. Ma, T.; Bhushan, B.; Murooka, H.; Kobayashi, I.; Osawa, T. A. Rev Sci Instrum 2002, 73, 1813.
10. Ma, T.; Bhushan, B. J Appl Polym Sci 2003, 89, 3052.
11. Ma, T.; Bhushan, B. J Appl Polym Sci 2003, 88, 2082.
12. Ma, T.; Bhushan, B. J Appl Polym Sci 2003, 89, 548.
13. Chen, D.; Zachmann, H. G. Polymer 1991, 32, 1612.
14. Owners Manual for the Rheometrics RSA-II Dynamic Mechanical Analyzer, Rheometrics, Inc., 1-T Possumtown Rd., Piscataway, NJ 08854-9990, (201) 560-8550.
15. Ward, I. M.; Hadley, D. W. An Introduction to the Mechanical Properties of Solid Polymers; Wiley: New York, 1993.
16. ASTM 882-97, ASTM E831-93, and ASTM D696-98. Annu Book ASTM Stand 1993; 1997, 14.02:348–351; 1999, 8.02:85–88.
17. Jones, R. M. Mechanics of Composite Materials, 2nd ed.; Taylor & Francis: Philadelphia, 1999.
18. Ferry, J. D. Viscoelastic Properties of Polymers, 3rd ed.; Wiley: New York, 1980.
19. Silva, M.; Spinace, M.; Paoli, M. J Appl Polym Sci 2001, 80, 20.
20. Haghighat, M. K.; Borhani, S. J Appl Polym Sci 2000, 78 1923.
21. Gillmor, J. R.; Greener, J. SPE ANTEC 1997, 45, 1582.
22. Kumar, S. G.; Kumar, R. V.; Madras, G. J Appl Polym Sci 2002, 84, 681.
23. Ouchi, I.; Hosoi, M.; Tomie, T. Jpn J Appl Phys 1992, 31, 2505.